Phytochemical Screening, Formulation and Optimization of Ehretia Laevis Loaded Silver Nanogel

Imran Jameel Syed

imranpharm07@gmail.com

SBSPM's B. Pharmacy College

Rana Zainuddin Ahmed

Y. B. Chavan College of Pharmacy

Research Article

Keywords: Nanogel, Ehretia Laevis, Flavonoids, LC-MS QTOF, Antioxidant

Posted Date: November 12th, 2025

DOI: https://doi.org/10.21203/rs.3.rs-7883244/v1

Additional Declarations: No competing interests reported.

Version of Record: A version of this preprint was published at Journal of Pharmaceutical Innovation on March 4th, 2026. See the published version at https://doi.org/10.1007/s12247-025-10274-3.

Abstract

Purpose

The purpose of this study was to prepare, characterize, and optimize an Silver Nanoparticle loaded nanogel(AgNP) through the ethyl acetate fraction of *Ehretia laevis* leaf extract through the green synthesis system to heal topical wounds better, particularly problems in permeation and sluggish inflammation in chronic wounds.

Method

Phytochemical screening was used to verify that the extract had flavonoids, phenolic compounds, and triterpenoids. Green method was used to prepare AgNPs, which were optimized through a 3-level factorial design in order to obtain the desired size of the particle, zeta potential and solubility. UV-Vis spectroscopy, FTIR, LC-MS QTOF (detecting 28 bioactive compounds), FESEM (morphology) and XRD (crystallinity) were used as the methods of characterization. The optimized AgNPs were placed in a carbopol-based gel where they were tested in terms of physicochemical characteristics (pH, viscosity, spreadability), drug release, antimicrobial activity, and antioxidant potential.

Results

The optimized AgNPs had an average hydrostatic diameter of 103.4 nm, zeta potential of -28.7 mV, a solubility of 0.877 mg/mL, a round shape, crystalline structure, and a 97.54 percent solubility of drug. The nanogel exhibited optimal properties: PH 7, viscosity 3655 cps, spreadability 3.1g.cm/s and drug release 97.54%. The *Ehretia laevis* phytochemical synergies and AgNPs were found to improve antimicrobial and antioxidant effects.

Conclusion

The *Ehretia laevis* AgNP-loaded nanogel is a potentially suitable therapy in topical wound healing because of its better physicochemical, release, and bioactivity characteristics. Efficacy and safety needs additional in vivo and clinical trials to prove.

1 INTRODUCTION

Wound healing is a complicated physiological process with a sequence of cellular and molecular activities such as hemostasis, proliferation, inflammation, and tissue repair to restore skin integrity to injured skin[1].Effective wound healing formulations should be developed, which will accelerate this process and prevent infections and regenerate tissues with the delivery of bioactive agents in a targeted and controlled manner. The drugs of this type might be gels, ointments, or nanogels and frequently include antimicrobial and anti-inflammatory substances to solve problems, such as chronic wounds, microbial infections, etc[2].Out of these, nanoparticle-loaded nanogels have proved to be advanced carriers, and these systems are associated with better drug delivery, better penetration and prolonged delivery required to achieve the best wound healing results. Chronic wounds, diabetic ulcers, or burns exert deformations on the physiology of wound healing, resulting in protracted

inflammation or inhibition of angiogenesis or infection susceptibility[3]. These disorders are marked by defective regulation of cellular functions such as excessive oxidative stress, impaired collagen production, and continual microbial colonization, and slowing of tissue healing processes.[4].

The difficulties associated with drug delivery that inhibit effective disease targeting in wound healing include poor penetration into the skin barrier, poor retention in the wound area, and lack of controlled release to achieve the prolonged beneficial effects [5, 6].Creams or ointments are examples of conventional formulations that cannot be efficient in conveying active agents, such as antimicrobials or anti-inflammatory drugs, to the deeper layers of the damaged tissue, and thus result in suboptimal outcomes when it comes to managing chronic wounds. The solution lies in nanoparticle-based delivery systems, especially nanogel based systems that will not only stabilize the drug and facilitate its penetration to the tissues but will also allow targeted and prolonged release at the wound site. The skin, which is the biggest affected organ in diseases of wound, undergoes physiological issues, including the decreased barrier mission, less vascularization, and immune reactions, worsening the delay in wound healing[7].In long term injuries, matrix metallo proteinases are increased, and the extracellular matrix of the skin is degraded, in addition to the fibroblast activity being disturbed by the unremitting inflammation effecting tissue regeneration. These pathological defects in the physiology require more enhanced formulations with the responsibility of attending to the antimicrobial requirements along with the resurrection of skin functionality. These problems can be managed through the use of nanogels loaded with bioactive nanoparticles to achieve two outcomes: repairing tissue and fighting infection around the wound. A number of products have been developed to treat the wound-related diseases in the marketplace; this includes silver-based dressings such as Acticoat andSilvercel and hydrogels such as Intrasite Gel, Nu-Gel which have antimicrobial activity and a wet wound environment[5]. The products have found extensive application in clinics to treat acute and chronic wounds by ensuring no infection risks and to aid in tissue hydration. Nevertheless, their marketed formulations have several limitations, i.e., low penetration into the deeper layers of the wound, a short drug release profile, and very poor capacity to overcome the complicated physiology of the wound, like extensive inflammation or oxidative stress [2, 8].As an example, it is easy to assume that silver dressings exhibit silver ions at a rate which would prove cytotoxic, and hydrogels have no mechanical strength or desirable target delivery which is vital to chronic wounds.

In order to overcome these constraints, Novel drug delivery systems(NDDS) such as loading of nanogels with silver nanoparticles (AgNPs) can be constructed to offer prolonged and controlled drug release, improved penetration kinetics, and multiple effects on curative effects [9].By integrating AgNPs with additional potent antimicrobial and anti-inflammatory properties into nanogels, the systems can enhance the drug retention in the wound site and minimize cytotoxicity by controlled drug release as well as overcome physiological hindrances, such as oxidative stress and inflammation. Also, by optimizing the formulations of nanogels, i.e., using statistical design, i.e., Box-Behnken, one can improve the physicochemical characteristics of the nanogels such that they can improve stability, entrapment efficiency, and tissue compatibility. It has been indicated that other places have reported the use of plant-mediated AgNPs and nanogels in wound healing applications. As an example, showed synthesis of AgNPs with the help of *Ehretia laevis* leaf extract and characterised them by their antimicrobial and photocatalytic activities, but did not look at their further inclusion into nanogel[10].Wadher.etal (2021) developed nanoemulgel with topical optimized Pongamia pinnata extract with an increased depth of penetration and responses to antimicrobial activity. Some reports have also indicated the use of AgNP-loaded nanogels with various plant extracts, including *Azadirachta indica*, in the healing of wounds, in which the utilization of these particles is being found to be capable of fighting infection and aiding tissue regeneration as

well[11].Yet, their works tend to lack thorough phytochemical screening or organized optimization of nanogel constructs in relation to *Ehretia laevis*-derived AgNP.

AgNPs have proven to be a valuable therapeutic mrdication in wound amplification, as they exhibit broad-spectrum antimicrobial activity because of their capacity to break down the cell membranes of bacteria, as well as their inflammatory dampening impact by mediating cytokine manufacture[12]. AgNPs have a promising role in killing multidrug-resistant pathogens and characterizing chronic wounds, like Pseudomonas aeruginosa and Staphylococcus aureus. AgNPs have high therapeutic value with minimal toxicity when enclosed in nanogels; they give sustained release qualities with high therapeutic efficacy. The biocompatibility of AgNPs is improved by using plant extracts, like that of *Ehretia laevis*, which makes AgNPs compatible to use as a topical preparation for wound-related diseases.AgNPs have received great attention as a wound-healing drug. To give an example, Tian et al. (2007) exposed animal models to AgNPs and showed that the levels of inflammation were decreased, and wound closure was accelerated due to enhanced keratinocyte proliferation. Equally, Kwan et al. (2011) prepared AgNP-loaded hydrogels exhibited more potent antimicrobial potential and better wound healing potential on infected wounds [13]. Plant-mediated AgNPs, which include *Aloe vera* synthesized AgNPs, have been studied, and wound contraction and collagen deposition were improved when those AgNPs were applied to the wound [14].

Exerting drug delivery and disease effect in wound healing, the choice of AgNP-loaded nanogels engineered with extract of *Ehretia laevis* has several merits. First, the nanogel matrix gives a regulated and long-term release behavior of AgNPs, improving the retention of medication at the wound location and low systemic toxicity relative to traditional silver dressings [9].Secondly, the nanoscale of AgNPs (normally 10-100nm) drives further penetration of the skin layers, where infection and inflammation are treated at the cellular level. Third, the phytochemicals present in *Ehretia laevis* extract (e.g., flavonoids/phenols) are nature-derived reducing and stabilizing agents that enhance the antioxidant ability and biocompatibility of the AgNPs that reverse oxidative stress-mediated chronic wounds.[10].In contrast to current treatment modalities, this formulation bypasses the physiological impediments of chronic wounds by reducing microbial burden, modulating the inflammatory response, and stimulating tissue regeneration, therefore providing a better alternative to existing therapies.

Although the *Ehretia laevis*-mediated AgNPs can hold a lot of promise, very few studies have been conducted to examine its phytochemical constituents in either nanoparticle production or the incorporation of nanoparticles in nanogels to treat wounds. Further, nanogel formulations have not been systematically optimized in order to maximize entrapment efficiencies, stability, and the kinetics of release. This research would aim to fill these research gaps by carrying out phytochemical screening of *Ehretia laevis* leaf extract, synthesis of AgNPs through a green methodology, preparation of an AgNP-loaded nanogel, and optimization of characteristics of the nanogel in terms of its drug delivery capacity as well as it’s wound healing activity.

2 Material and method

2.1 Plant Material and Extract Preparation:

The *Ehretia Laevis* leaves were collected from the local residential area of Ambajogai and identified by the taxonomist of botanical survey of the India, Pune, having authentication number----------. The leaves were washed with water and dried at room temperature. The dried leaves were grinded in a mixture to make the

powder. The fine powder of leaves (200g) was subjected to extraction with 70% ethanol for 48 hours by using a soxhalate apparatus to get the hydroalcoholic extract at 55℃[15].For ethyl acetate fractionation, 5g of viscous extract was inserted into a mortar with warm distilled water, then stirred to form a suspension and transferred into a separating funnel. The extract suspension was added with ethyl acetate (1:1) and shaken to form two layers. The ethyl acetate soluble fraction above was taken and then filtered over Whatman No.1 paper as filtrate I using Büchner funnel. While the ethyl acetate unsolved fraction was refractionated with ethyl acetate two times until obtained filtrate II and III. The ethyl acetate soluble fraction was collected and then evaporated by a Büchi rotary evaporator at 60°C[16].

2.2 Phytochemical screening:

Various phytochemical testswere performedto confirm the presence of phytoconstituents like flavonoids, phenols, and terpenoids within the extract.

2.3 LC-MS Q-TOF Analysis of Metabolites[17]

Sample Preparation and Injection

Sample injections 3 µL were performed with the Agilent HiP Sampler (G4226A) with a draw/eject speed of 100 µL/min and needle wash (3 s, flush port) to avoid carry over Correct sampling was done by vial bottom sensing.

Liquid Chromatography:The separation was carried out through Agilent Binary Pump (G4220B) at 0.3 mL/min on a column heated at 40 o C (G1316C). The mobile phase was 0.1% formic acid in water (A) and methanol (B), and gradient: 95% at 1 min and 0% at 2530 min was 95% A/5%B. The total run time was 35 min.

UV-Vis Detection

A Diode Array Detector (G4212B) monitored absorbance at 230, 254, 269, and 280 nm (4 nm bandwidth), with spectra recorded from 190–600 nm (2 nm step). The reference wavelength for 230 nm was 360 nm (100 nm bandwidth).

MassSpectrometry: An Agilent Q-TOF MS (G5550A) with Dual AJS ESI in positive mode was used. MS scans (120–1200 m/z) and MS/MS were acquired at 1 spectrum/s. AutoMS2 selected up to 10 precursors/cycle (threshold: 10,000 counts, 0.010% relative) with ramped collision energies (charge 1: slope 8, offset − 2.6; charge 2: slope 6, offset − 2.6; charge 3: slope 4, offset − 2.6). Source parameters included gas flow (13 L/min), sheath gas (300°C, 11 L/min), gas temperature (250°C), nebulizer (35 psig), capillary voltage (3500 V), and fragmentor (175V). Active exclusion was enabled (1 spectrum, release after 0.2 min), and mass 197.8075 was excluded. MS data collection stopped at 30 min.

Data Acquisition

Total ion chromatograms (TIC) and MS/MS spectra were recorded for analysis. The method was optimized for untargeted metabolite profiling with high sensitivity and reproducibility.

2.4 Preparation and optimization of Silver Nanoparticle of *Ehretia Laevis*:

A green synthesis method was used where the extract was incorporated into a mixture of deionized water and silver nitrate, which was kept in the dark for 24h, and change in colour of the solution, confirmed the formation of AgNPs. The mixture was centrifuged at 15000 RPM for 30 minutes, and the particles that settled down were collected and washed thrice with deionized water[18].

2.4.1Factorial design

In Stat Ease design expert software version 12, the optimization and selection of the batch with the sound effect were done using a 3^2- level factorial design. In the Silver nanoparticles, the concentration of silver nitrate (A) and the time(B) would have different levels in (-1,0,+1) of each, as indicated in Table 01. Particle size, solubility, % drug release and % yield were the dependable variable studies. To achieve the optimization of formulation through the application of experimental design, nine batches of each of the formulations have been prepared. The reaction was monitored with varying levels of silver nitrate 1mM, 2mM and 3mM and at intervals 8h, 16h and 24h.

Table 1
Composition of EAFEL Silver nanoparticle

Composition	F1	F2	F3	F4	F5	F6	F7	F8	F9
EAFEL(mg)	500	500	500	500	500	500	500	500	500
AgNo3(mM)	1	2	3	1	2	3	1	2	3
Time(h)	8	16	24	8	16	24	8	16	24
AgNO3:Time	1:8	2:16	3:24	1:8	2:16	3:24	1:8	2:16	3:24

Table 2
Factorial studies for *Ehretia laevis* silver nanoparticle

Factor	Name	Level(-1)	Level(0)	Level(1)
A	Concentration of silver nitrate	1mM	2mM	3mM
B	Time	8h	16h	24h

2.5 Charactrization of silver nanoparticles

2.5.1 UV

Qualitative analysis to examine the production of EL-AgNPs from ELEA fractionation was done spectro photometrically. This technique depends on seeing color changes, particularly when an EAFEL reduces $AgNO_3$. The reaction was allowed to continue for 24 hin accordance with the synthesis procedure that was stated, and then the presence of a dark brown colour was visually examined. The effective formulation of EL-AgNPs was revealed by the appearance of this colour. A tiny amount of the reaction mixture was put in a cuvette once the dark brown tint was seen. An EL-AgNPs sample was measured using a UV-Vis spectrophotometer and scanned between 200 and 800 nm with a 1 nm interval. This wavelength range is the target absorbance range of EL-AgNPs. Finally, the outcomes were compared with the already published spectrum peak values [19–21].

2.5.2 Fourier transforms infrared spectroscopy analysis

FTIR proved useful in confirming the existence of functional groups. The Agilent Technologies FTIR spectrophotometer was used to record the nanogel formulation's FTIR spectrum. The range of 4000 to 650 cm^{-1} was used for the scan[22, 23].

2.5.3 Particle size:

Particle size was determined using a HORIBA SZ-100 nanoparticle size analyzer. The nanogel was mixed with some distilled water and loaded in the sample holder for analysis. The particle size analyzer works using laser diffraction to measure particles that are between 1 and 10,000 nanometers[23, 24].

2.5.4 Zeta Potential

Measurement of zeta potential of diluted samples was performed using a zetasizer (HORIBA SZ100, Japan).The beaker with the 1 mm formulation was combined with 9 mm of the distilled water. We used clear cuvettes to put the samples in and recorded the results later. The surface charge and the zeta potential are both obtained on the nanoparticle. Depending on the size of the zeta, stability tests can be carried out potential formulation [25, 26].

2.5.5 X-ray diffraction (XRD spectra):

The XRD was done by using smart lab JapanSpectra, which hasdiffractometer(Bruker D8 Advance diffractometer), to gather X-ray diffraction data of synthesized silver nanoparticles. For this Nickel-filtered Cu Kα radiations were used to record data at 30°C, 40kV voltage, and at 30mA current[27].

2.5.6 Scanning electron microscopy-Energy dispersive X-ray Spectroscopy (FESEM-EDAX):

ELSNPs shape and morphology were measured by scanning electron microscope Quanta 200 with an Energy Dispersive X-Ray (EDAX) Spectrometer (Netherlands). The high vacuum mode analysis was carried out following the deposition of the nanoparticles on the EM stubs and sputtering of the same using gold to provide conductivity[28].

2.6 Solubility Study of ELSNPs

The experiment determined the solubility of EL-AgNPs in water by following the WHO specification from July 2018 (QAS/17.699/Rev.2). To test for solubility, the "shake flask" method was employed. An excessive amount of the silver nanoparticles was added to screw-capped vials that had already been filled with 5 mL of distilled water in order to conduct the experiment in triplicate.

After that, the vials underwent three cycles of ultrasonication for five minutes each, separated by fifteen minutes. A vortex shaker was used to further mix the fluid until saturation was achieved. To reach saturation equilibrium, the vials were then placed on an orbital shaker with an ideal agitation rate and left undisturbed for 24 hours at 37℃ ± 1℃.Whatman filter paper number 41, which has pores of 0.45µm, was used to filter the samples. Following a suitable dilution with distilled water, the filtered samples were subsequently subjected to spectrophotometric analysis at 437 nm using the established method. A UV spectrophotometer was used to test the samples' absorbance, and the solubility (mg/mL) was determined. The results are presented in Table 08[29, 30].

2.7 Permeability study

A Franz diffusion vertical cell (Thermo Fischer Scientific, Haake S5P Newington, USA) with a diffusion area of 5.024 cm^2 (capacity 14mL) was used to investigate the permeability of EL-AgNPs. The egg membrane is positioned between the donor and receptor compartments in the Franz diffusion cell configuration. To guarantee sink conditions, 8mL of physiological saline solution (pH 7.4) combined with methanol in an 8:2 ratio was placed inside the receptor compartment. The solution was kept at a steady temperature of 37 ± 0.5℃ while being constantly swirled at 400–500 rpm. Following the application of the EL-AgNP (10 mg) formulation to the donor compartments, the receiving solution was progressively changed out for a new solution at predetermined intervals, making sure that it was totally drained prior to each sampling. Aliquots were then filtered and examined using a UV-Vis spectrophotometer set at 437 nm.

2.8 Preparation and optimization of *Ehretia Laevis* Nanogel

EL-AgNP-loaded hydrogel was created by simply combining the AgNPs into a premade hydrogel matrix. To create a homogenous hydrogel, the polymer was dissolved in deionized water and constantly agitated to create the Carbopol gel base. After that, the hydrogel's volume was changed to produce three distinct strengths: 0.5%, 1.0%, and 1.5%. Then slowly added 1 gm of PEG to the water and Carbopol mixture, stirring is continued until it got completely dissolved. Triethanolamine was added drop by drop while monitoring the pH. After each addition, mix well and check the pH. Once the gel reaches the desired pH and consistency, stop adding triethanolamine .Dissolve 0.02g Methyl Paraben and 0.01g of Propyl Paraben in a small amount of warm water and mix into the gel. Incorporate the ELAgNPsdispersion (quantity depends on desired concentration, (e.g., 10-50ppm). Add water (QS) to make the total weight 10g.

Table 3
Formula for EAFEL Silver Nanogel.

Sr No	Ingredient	ELG1	ELG2	ELG3
1	ELSNPsparticles	0.1 gm	0.1 gm	0.1 gm
2	Carbapol940	0.05gm	0.1gm	0.15gm
3	PEG600	1gm	1gm	1gm
4	Triethanolamine	0.05–0.1 gm	0.05–0.1 gm	0.05–0.1 gm
5	Methyl parabene	0.02 gm	0.02 gm	0.02 gm
6	Propyl parabene	0.01 gm	0.01 gm	0.01 gm
7	Distilled water	QS to 10gm	QS to 10gm	QS to 10gm

2.9Evaluation of gel

2.9.1 Physical characteristics and PH

The hydrogel's physical characteristics, such as its colour, homogeneity, consistency, and phase separation, were visually assessed. An NIG333 digital pH meter was used to measure the hydrogel's pH. After inserting the pH meter's glass electrode into hydrogel, the pH was measured.Three duplicates of each experiment wereconducted[31].

2.9.2 Viscosity

A Labman LMDV-60 viscometer was used to measure the hydrogel's viscosity at room temperature. After being put in a beaker, the hydrogel (30 g) was left to equilibrate for 10 minutes. Using spindle number four, angular velocity runs were conducted at 6, 12, 30, and 60 rpm. For every speed, the viscosity in millipascal seconds (mPa s) was shown on the screen. At room temperature, three separate observations were made[32].

2.9.3 Spreadability

A topical gel should have a high enough spreading coefficient—this slide—before it is applied or rubbed onto the skin's surface. The gel was then spread out at a precise distance and sandwiched between the two glass slides by adding 500 g of mass to the slide that was placed above it.The timetaken for the gel to shift that far from its starting position was noted[23, 33].

3 RESULTS

3.1 Phytochemical investigation of *Ehretia laevis*.

The presence of flavonoids and phenolic compounds in the EAFEL was confirmed by phytochemical tests.The results suggested that the EAFEL contains the high number of flavonoids and phenolic compound present in the ethyl acetate fraction (Table: 4).

Table 4
Phytochemical present in EAFEL

Sr no	Test	Observation
1	Flavonoids	Present^{+++}
2	Phenols	Present^{+++}
3	Terpenoids	Present^{++}
4	Protein	Absent
5	Tannins	Present^{+}

The UV/Vis absorption spectrum of EAFEL shows strong absorbance at 283nm,and the RfValuewas found to be 0.90.Melting point of the fraction was found to be 190°C. The λmax value shows the compound must contain the phenolic compounds or flavonoid, which has an absorbance range in between 250 and290nmfrom the test, it was noticed that the plant contain large amount of flavonoids.

3.2 UV-Visible Spectroscopy:-

One of the useful methods of structural characterization and stabilization of silver nanoparticles is UV-Vis spectroscopy. It is established that silver nanoparticles are supposed to have a peak maximum UV-vis absorption at the range of 300-500nm..Depletion of pure Ag + ions to Ag0 was tracked through the measurement of the spectrum of the reaction media at a time interval. In our current study, silver surface plasmon resonance occurred at 438nm with a shift seen in the maximum wavelength. The reason why the intensity might increase is because the number of the nanoparticles formed must have been increased because of a decrease in the

amount of silver ions present in the aqueous medium. a previous report had established that the maximum absorbance was the result of the presence of the silver particles [34].

3.3 Fourier-transform infrared spectrometric analysis

Figure 5 IR Spectra of Silver nanoparticle gel of EhretiaLaevis

FTIR spectrum of the EAFEL leaf extract (Fig. 3) revealed the occurrence of several key functional groups associated with bioactive secondary metabolites.

Table 5
IR Spectral Analysis of Ehretialaevisethylacetate fraction

Wave number	Vibration type	Functional group	Likely phytochemical
3400	O-H Streching	Hydroxyl	Phenolic compound,Flavonoids
2925	C-H Streching	Alkanes	Triterpenoids, Fatty acids
1720	C = O Streching	Carbonyl(ester/acid)	Phenol,flavonoids
1610	C = C Streching	Aromatic ring	Flavonoids, Phenolic compounds
1050	C-O Streching	Alcohol	Flavonoids

These peaks suggest the presence of flavonoids, phenolic compounds, and possibly triterpenoids.The FTIR spectrum of AgNPs synthesized using the ethyl acetate fraction of *E. laevis* (Fig. 4) showed slight shifts and intensity changes in absorption bands compared to the crude extract, indicating the interaction of phytoconstituents with the nanoparticle surface.

Table 6
IR Spectral Data for Silver Nanoparticles Synthesized with Ethyl Acetate Fraction of *Ehretialaevis*

Wave number	Vibration type	Functional group	Role in Nanoparticle Synthesis
3350	O-H Streching	Hydroxyl(Phenolic/alcoholic	Reduction and capping
2900	C-H stretching	Alkane	Capping
1650	C = O stretching	Carbonyl (acid/ester)	Capping and stabilizing
1030	C-O stretching	Alcohol/ether	Capping

3.4 LC-MS (QTOF) of EAFEL

The analysis of the ethyl acetate fraction was done by using LC-MS/QTOF.Table 7 represents the information of peaks observed during the analysis. LC-MS analysis shows the presence of 28 phenols. The table below lists the active compounds along with their molecular formula, molecular mass (mass), retention time (RT), and m/z ratio (mass-to-charge ratio)(Table 7).

Thecompatibility of the drug polymers used in the formulation was also confirmed by FTIR analysis, which ensures the stability of the components of the formulation in gel.

Table 7
Compounds identified in ethyl acetate fraction of *Ehretia laevis* by LC MS –Qtof

Sr No	Retention time	Molecular Weight	Compound Name	Molecular Formula	M/Z ratio
1.	10.119	382.1976	Cinncassiol C3	C20 H30 O7	405.1868
2.	9.393	286.0449	Maritimetin	C15 H10 O6	287.0518
3.	8.336	594.1534	Kuwanon Z	C34 H26 O10	595.1609
4.	24.108	526.2551	Withangulatin A	C30 H38 O8	549.2443
5.	26.286	512.2758	Ganosporelactone A	C30 H40 O7	535.2652
6.	8.194	483.2317	N1-Caffeoyl-N10-feruloylspermidine	C26 H33 N3 O6	484.2388
7.	9.571	497.2476	N1,N10-Diferuloylspermidine	C27 H35 N3 O6	498.255
8.	7.164	214.0291	Dibenzo[1, 4]dioxin-2,3-dione	C12 H6 O4	237.0187
9.	10.611	140.0478	Gentisyl Alcohol	C7 H8 O3	163.037
10.	11.989	270.0511	Aloe-emodin		269.0437
11.	11.685	716.136	Theaflavin-3-gallate	C36 H28 O16	715.1282
12.	9.997	718.1511	Salvianolic acid L	C36 H30 O16	717.1441
13.	10.536	360.0838	Chrysosplenol D	C18 H16 O8	359.0765
14.	9.989	720.168	Sagerinic acid	C36 H32 O16	719.161
15.	8.521	178.0257	7,8-Dihydroxycoumarin	C9H6O4	177.0184
16.	9.502	538.1102	Isomelitric acid A	C27 H22 O12	537.1029
17.	9.811	508.1004	1,2,4,7-Tetraacetoxy-8-hydroxy-3-(4-hydroxyphenyl)dibenzofuran	C26H20O11	
18.	7.159	110.036	Resorcinol	C6H6O2	109.0288
19.	7.237	154.0258	2,6-Dihydroxybenzoic acid	C7H6O4	153.0186
20.	6.922	198.0523	Vanillylmandelic acid	C9 H10 O5	197.045
21.	6.933	350.0997	3-Feruloyl-1,5-quinolactone	C17 H18 O8	395.098
22.	6.29	192.0626	Quinic acid	C7 H12 O6	191.0554
23.	6.768	506.1059	Tricin 7-glucuronoside	C23 H22 O13	551.1044
24.	6.93	168.041	Vanillic acid	C8 H8 O4	167.0339
25.	6.93	180.0415	Monomethyl phthalate	C9 H8 O4	179.0342
26.	10.802	196.0724	1-(2,4,5-Trihydroxyphenyl)-1-butanone	C10 H12 O4	195.0652
27.	10.54	350.0545	Dehydrogriseofulvin	C17 H15ClO6	395.053

Sr No	Retention time	Molecular Weight	Compound Name	Molecular Formula	M/Z ratio
28.			Lilalin		

The high- resolution LC-MS (QTOF) identified the 28 component (Table 7), which belong to phenolic compounds, flavonoids, terpenoids, organic acids, etc. From the obtained result, it was observed that a large amount of polyphenolic compounds are present in the EAFEL leaves .A detailed characterization of phenolic composition and other minor phytochemicalswas accomplished for the first time by using LC-MS. This resulted in the identification of 28 phenolic compounds.Although many studies were carried out before this study by using GC-MS, the different parts were used for the studies.Rangnathrao et.al studied the GC-MS of hydroalcoholic extract of *Ehretia laevis* flowers,which were fractioned by different solvents like n-hexane and ethyl acetate.45 different compounds had been identified, but it did not clarify which portion of solvent contained which compounds[35]. In another study, Rasika C Torane et.al. studied the GC-MS of *Ehretia laevis* leaves.They used the n-hexane as solvent, and they obtained the 11 major components which are alcohol,aliphatic, hydrocarbons, and fatty acids and aromatic esters. The remaining ones are hydrocarbons, whereas two of them are oxygenated[36]. Joshi etal. studied the GC–MS study of bark of the *Ehretia laevis* by using the different solvents like petroleum ether,chloroform and methanol and found 13,17 and 19 compound respectively[37].In the present study we have used the ethyl acetate, which confirms the large number of phenolic compounds that were not confirmed till now (Table 1) the different flavones flavans are also confirmed by the LC_MS study.

3.5 Optimizationof Silver nanoparticles:-

Preliminary research was conducted to determine the maximum and lower limits of the silver nitrate concentration and time using a trial-and-error method based on the silver nanoparticles' size, solubility, percentage of drug release, and yield. The lower limit for silver nanoparticles was found to be 1mM and the upper limit was found to be 3mM and time in 8h, 16h and 24h as critical limit mentioned in above Table 01For final optimization of formulation and in-depth investigation of the effect of independent variables on responses was done by experimental design technique 3level factorial on DOE software. The factorial study was carried out to find a significant effect of the most influencing factors; those are the different concentrations of silver nitrate and time on responses including particle size,solubility,percentage drug release, and percentage yield. The final optimum formulation batch was chosen after a study was conducted to determine the optimal amounts of independent factors. Each silver nitrate concentration was used in nine batches, and all of the answers were recorded and fitted to a separate model. We determined the ideal level of an independent variable based on that. Numerous polynomial equations were found in optimization research, as Table 01 illustrates. Of additional A synergistic impact is shown by a positive sign, while an antagonistic effect is indicated by a negative sign.[38]. The varying concentrations of the silver nitrate at varying times influence the size, solublility and the percent release of the drug that is graphically represented by the response surface curve as shown in Fig. 06 Effect of independent variables on various parameter, FirstlySolublity: the 3D surface plot shows the correlation between AgNO3 concentration, time and the percent release of the drug. The solubility increases with increasing $AgNO_3$ concentration up to approximately 2.0 mMol and with time up to about 16h, reaching a maximum of approximately 0.67 mg/mL. Beyond these points, solubility starts to decrease, with the lowest values observed at the extremes, such as 1 mMol $AgNO_3$ and 8h (around 0.27 mg/mL). The surface forms a curved, saddle-like shape, indicating a non-linear relationship, with a peak solubility region rather than a uniform increase or decrease with either factor. The design points, marked with red and pink circles, show the actual experimental

data, scattered across the surface, suggesting multiple measurements to map the response."The 3D surface plot of shows that the percentage drug release varies with both $AgNO_3$ concentration and time. The maximum drug release, approximately 94.85%, is observed at an $AgNO_3$ concentration of about 2mMol and a time of around 16h. The surface plot indicates that drug release increases as $AgNO_3$ concentration increases from 1 to approximately 2 mM and time from 8h to 16h, reaching a peak, and then slightly decreases at higher values of these factors, with the lowest releases (around 84–86%) at the extremes, such as 1 mM $AgNO_3$ with 24h or 3mM with 8h. The surface forms a curved plane, suggesting a non-linear relationship, with a peak region rather than a uniform increase or decrease. The design points, marked with red (above surface) and pink (below surface) circles, are scattered across the plot,The 3D surface plot reveals that particle size varies non-linearly with $AgNO_3$ concentration and time. The minimum particle size, approximately 190 nm, is observed at around 2 mM$AgNO_3$ and 16h. Particle size increases at the extremes, reaching up to 532 nm at 3mM $AgNO_3$ with 24h or 1 mM with 8h. The surface exhibits a saddle-like shape, indicating an optimal region, with design points scattered above and below the surface, reflecting experimental variability. The 3D surface plot demonstrates a non-linear relationship between $AgNO_3$ concentration, time, and percentage yield. The maximum yield, approximately 87%, is observed at around 2mM $AgNO_3$ and 16h. Yield decreases at the extremes, dropping to about 58% at 1 mM with 24h or 3mM with 8h. The surface shows a peak region, with design points scattered above and below,

Table 8
Evaluation results for optimization batches of EAFEL silver nanoparticles

RUN	Factor 1A:AgNO3MMol	Factor 2B:TimeHrs	Response 1Solublity(mg/ml)	Response 2Drug release(%)	Response 3 Yeild(%)	ResponseParticle size (nm)
1	1	24	0.76598	90.0478	70	207.6
2	2	24	0.73998	90.62	67	260.1
3	3	8	0.62598	88.51	67	340.2
4	2	16	0.876598	95.54	87	103.4
5	1	8	0.371998	84.86	58	391.1
6	1	16	0.709198	91	83	207.6
7	2	8	0.543198	84.67	62	320.6
8	3	16	0.573198	94.8478	80	141
9	3	24	0.636598	90.43	62	301.6

Table 9
Evaluation results for optimization batches of EAFEL nanoparticles

Formulation	Solublity(mg/ml)	Drug Release (%)	Yield (%)	Particle size(nm)
F1	0.371998	84.86	58	391.1
F2	0.543198	87.67	62	320.6
F3	0.62598	88.51	67	340.2
F4	0.709198	91	83	207.6
F5	0.876598	97.54	87	103.4
F6	0.573198	94.8478	80	141
F7	0.76598	90.0478	70	207.6
F8	0.73998	90.62	67	260.1
F9	0.636598	90.43	62	301.6

The above table shows the results of different batches, by which we can select the perfect batch formed, and from the above results, the design of the experiment also suggests the optimized formula for the formulation of perfect nanoparticles the DOE suggest the results for the optimized batch are shown in the below Table 10 and from the observation it was found that the F5 batch has more optimized nanoparticles having a size of 103.4nm, and due to this low size there is an increase in solubility, and drug release was observed, and the yield obtained at this concentration of silver nitrate and time was 16 hrs showing the optimized batch.

Table 10
optimized results for EAFEL nanoparticles

AgNO3	Time
2	16

3.6 Dynamic light scattering (DLS) analysis:

Figure 6A **Particle Size Analyses**

3.6.1 Particle size

The Dynamic Light Scattering (DLS) analysis in aqueous solution was used to establish the particle size, zeta potential, and dispersivity of the nanoparticle. The finding showed that the average size of silver nanoparticles of Ehretialaevis was 102.4nm.

3.6.2 Zeta Potential

Zeta potential of ELAgNO3 Nanoparticles was − 28.7mV.

3.7 FESEM-EDX:

Field Emission Scanning Electron Microscopy (FESEM) was performed to characterize the morphology and size distribution of AgNPs synthesized using the ethyl acetate fraction of *Ehretia laevis* leaf extract. The FESEM images (Figs. 3–7) revealed predominantly spherical AgNPs with a size range of approximately 40–80 nm. The nanoparticles exhibited a relatively uniform size distribution, consistent with the DLS mean particle size of 100.6 nm (SD 1.1 nm). Images 1–3 (Figs. 3–5) showed well-dispersed AgNPs with smooth surfaces, indicating effective stabilization by phytochemicals.

Energy-Dispersive X-ray Spectroscopy (EDX) was conducted to determine the elemental composition of AgNPs synthesized using the ethyl acetate fraction of *Ehretia laevis* leaf extract (sample ELSNP 02). The analysis, performed at 20 kV with a magnification of 600x, revealed the presence of silver (Ag), carbon (C), oxygen (O), silicon (Si), and chlorine (Cl) in Selected Area 2. The elemental composition is summarized in Table 11.

Table 11
Elemental composition for EL-AgNPs

Element	weight%	Atomic %	Net Intensity
C K	57.2	76.4	771.5
O K	19.6	19.6	233.4
Si K	0.6	0.3	82
Cl K	0.8	0.4	92.3
Ag L	21.8	3.2	914.4

The high carbon (57.2 wt%) and oxygen (19.6 wt%) content indicates a significant organic coating, while the silver content (21.8 wt%) confirms the formation of AgNPs. Trace amounts of silicon (0.6 wt%) and chlorine (0.8 wt%) were also detected.

3.8 X-Ray Diffraction

X-ray Diffraction (XRD) analysis was done to characterize the crystalline structure of silver nanoparticles (AgNPs) synthesized using the ethyl acetate fraction of *Ehretia laevis* leaf extract. The pattern exhibited prominent peaks at 38.1286°, 44.2628°, 64.4528°, and 77.3538° 2θ, corresponding to the (111), (200), (220), and (311) planes of the face-centered cubic (FCC) structure of silver, respectively.

3.9Solublity

It is crucial to research solubility since it has a direct impact on bioavailability. Drugs may not be absorbed effectively or reach therapeutic levels in the blood if they are not adequately soluble. But because they are more readily absorbed, highly soluble medications are more effective.Knowing how soluble plant extracts and EL-SNPs are will help determine how well they work as medication delivery vehicles. The hydroalcoholic extract's solubility in a comparative analysis was 0.384 mg/mL. On the other hand, 09 batches of EL-SNP formulations had solubility ranging from 0.3719 to 0.8765 mg/mL. The smaller size of particles improves the solubility. From the solubility study it was found that EL-AgNps formed at 1mMol concentration and 8hhave less solubility, as the proper nanoparticles are not formed, and the solubility also decreases at 3mM $AgNo_3$ at 24h due to increase in particle size at the concentration.

3.10Release study

The time dependency release pattern of EL-AgNPs that was synthesized in the presence of *Ehretia laevis* leaf extract exhibited a controlled pattern through more than one optimized batch. The in vitro drug release of *Ehretia laevis* silver nanoparticles (EL-AgNPs) was assessed across nine optimized formulations (F1–F9) to evaluate their release kinetics, a key determinant of therapeutic efficacy in nanogel applications. The cumulative drug release (CDR) percentage ranged from 84.86% (F1) to 97.54% (F5) over the study period. Formulation F1 exhibited the lowest release at 84.86%, suggesting a relatively slower release profile, potentially due to its larger particle size (391.1 nm) and lower solubility (0.372 mg/ml). Formulation F2 showed an improved release of 87.67%, while F3 achieved 88.51%, indicating a gradual increase in release efficiency. Formulation F4 demonstrated a notable release of 91%, reflecting enhanced dispersion (solubility 0.709 mg/ml) and a reduced particle size (207.6 nm). The highest drug release was observed in F5 at 97.54%, correlating with its smallest particle size (103.4 nm), highest solubility (0.877 mg/ml), and high yield (87%), suggesting optimal phytochemical-mediated stabilization (e.g., flavonoids identified at Rf = 0.90, UV = 283 nm) and surface area for release. Formulations F6 to F9 exhibited releases of 94.85% (F6), 90.05% (F7), 90.62% (F8), and 90.43% (F9), with F6 showing a high release close to F5, despite a larger particle size (141 nm). The progressive increase in drug release from F1 to F5, peaking at F5, highlights the influence of smaller particle sizes and improved synthesis conditions on achieving near-complete release, which is critical for sustained antimicrobial activity in the nanogel formulation.

3.11Preparation of *Ehretia laevis* silver nanogel

The gel was optimized on trail- and- error basis, and the formulated gel was subjected to the evaluation of parameter such as physical parameters, viscosity, spreadability, and % drug release were determined which were discussed in Table 12.

Table 12
Evolution of formulated Batches of EL-SNPs gel

Batches	Colour	PH	Apearence	Viscosity	spreadiablity	% drug release
F1G	Brown	6	Transparent	3241	2.6	93
F2G	Brown	6.7	Transparent	3293	2.8	95
F3G	Brown	7	3249	3655	3.1	97.54

Table 13
Evolution of Standard Drug

Sr No	Parameter	Observation
1.	Colour	White
2.	Apearence	Translucent
3.	Viscosity	3750
4.	Spreadiablity	3.1cm
5.	PH	7
6.	Percentage drug release	99.18%

3.11.1 Physical apearance and pH

The prepared gel of El-SNP was brownish in colour with a smooth and transparent apearence. The gel was found to be without any phase separation. The pH value of the formulated gel was found to be 7 the pH shows that the gel is physible with the human skin and considered safe for use [39]

3.11.2Viscosity

The important parameter of gel is Viscosity: the viscosity of gel is decreased with increased shear rate, while viscosity increases with an increase in the concentration of carbapol at different rpm. This could be attributed to the formation of a dense polymeric network at higher levels of polymer, as it facilitates the formation of connections between polymeric chains[40].Viscosity, measured in centipoise (cP), ranged from 3241cP (F1G) to 3293cP (F2G), with F3G showing the highest at 3655cP.

3.11.3 Spreadability

The spreadability of all the nanogel formulations ranged from 2.6 to 3.1g.cm/s. It was observed that formulationF3G showed higher spreadability, which may be due to an increased concentration of carbopol 940. While comparing with the marketed formulation, the spreadability of F3G gel was near to this gel, which was found to be 3750.

3.11.4In-Vitro drug Release of EL silver Nanoparticle gels

The percentage drug release was 93% for F1G, 95% for F2G, and 97.54% for F3G, with F3G demonstrating the highest release, aligning with its optimal particle size (103.4 nm) and solubility (0.877 mg/ml) from the corresponding F5 nanoparticle formulation.

4 Discussion

Phytochemical analysis of the *Ehretia laevis* leaf extract has shown a rich composition of bioactive compounds namely, the presence ofphenolic acids, flavonoids, pentacyclic triterpenoids, alkaloids, saponins, and tannins, suggesting its ethnomedicinal uses. The ethyl acetate extract, which was analyzed by thin-layer chromatography, showed a strong spot with Rf value of 0.90 corresponding to a moderately polar substance. UV-Vis spectroscopy of this fraction indicated peak absorption at 283 nm which matches with flavonoids or phenolic acids. A value like 0.90 is shown by using ethyl acetate: formic acid:glacial acetic acid:water solvent system indicates a

flavonoid, which is more likely to be quercetin or kaempferol, and is expected to be around 0.8–0.9 in these solvents [41]. The flavonoids are slightly polar in nature since they contain hydroxyl and glycosidic functional groups, as consistent with their extraction in ethyl acetate. Additional support for this identification can be drawn from the UV absorption at 283nm, as flavones and flavonols typically display type 2 transitions in the range of 250-300nm, with quercetin absorbing at 255 and 370 nm and kaempferol at 265–295 nm[42]. The presence of the peak at 283 nm indicates the flavonol with little conjugation or a phenolic acid like caffeic acid, which has an absorbance peak at around 280–320 nm. These findings are in alignment with those of Shukla et al. (2021), where flavonoids and phenolic acids were found to be some of the key components of *Ehretia laevis* leaves[43]. Comparatively, studies on related Boraginaceae species, such as *Cordia sebestena*, report similar phytochemical profiles, with TLC revealing flavonoids at Rf values of 0.85–0.95 in ethyl acetate-based systems. FTIR spectral analysis of the ethyl acetate fraction of *Ehretia laevis* leaf extract (Table 1, Fig. 1) and its derived AgNPs (Table 2, Fig. 2) provides critical insights into the phytochemical composition and the mechanisms underlying the green synthesis of AgNPs. The IR spectrum of the ethyl acetate fraction showed characteristic absorption bands at (3400cm -1 O-H stretching) (2925 cm -1 C-H stretching) (1720 cm -1 C = O stretching) (1610 cm -1 C = C stretching) and 1050 cm -1 (C-O stretching), suggesting the presence of phenolic compounds, flavonoids, and potential presence of triterpenoids[44]. These functional groups are in agreement with the descriptions of the phytochemical composition of *Ehretia laevis*, such as pentacyclic triterpenoids (e.g., betulinic acid, lupeol), phenolic acids, and flavonoids, e.g., quercetin that have shown anti-inflammatory and antioxidant activities[36]. The solvent extraction of ethyl acetate fraction in polar phytochemicals generates high value in AgNPs synthesis and to use these compounds enable reduction, stabilization. [10]. The IR spectrum of the AgNPs showed the bands appearing at 3350 cm O H stretching, 2900 cm C H stretching, 1650 cm C-O stretching and 1030 cm (C-O stretching and shifting), with decreased intensities, as compared to that of the ethyl acetate fraction, especially in the O-H and C-O stretching bands[10]. The IR spectra of the AgNPs revealed the bands at 3350 (O-H stretching), 2900 (C-H stretching), 1650 (C = O stretching) and 1030 (C-O stretching) cm^{-1} which were shifted and also overlapped in intensity as compared to the ethyl acetate fraction especially the O-H and C = O band shrunk in intensity[10, 45]. Such changes indicate that flavonoids and phenolic acids had a phenolic hydroxyl and carbonyl group that reduced Ag^{+} to Ag^{0} and capped the nanoparticle and inhibited aggregation [46]. The presence of an O-H band shift (e.g., 3400cm $^{-1}$ to 3350 cm^{-1}) suggests the coordination to the silver surface, whereas the decreased intensity of C = O bands indicates carbonyl group-containing compound-induced stabilization of AgNPs by improving its stability and bioactivity[47]. These interactions support the potential of *E. laevis* AgNPs for applications in nanogel formulations targeting antimicrobial and anti-inflammatory therapies[44]. Polar phytochemicals like flavonoids and phenolic acids of the ethyl acetate fraction may be attributed to effective AgNP synthesis over less polar fractions since polarity only separates those bioactive compounds holding the ability to reduce the silver ions[10, 44]. IR data also give support to this through the formation of a stabilizing coating that leads to an improvement in the potential of the AgNPs as antimicrobial, antioxidant, and anti-inflammatory compounds, as this was demonstrated by their activity against Culex quinquefasciatus larvae and cancer cell lines[10]. The presence of triterpenoids, such as lupeol, further supports the therapeutic potential of *Ehretia laevis* AgNPs for wound healing and anti-inflammatory therapies[48]. LC-MS QTOF analysis of the ethyl acetate fraction of the Ehretia laevis leaf extract showed a wide range of secondary metabolites (28 of them) represented by flavonoids (e.g., Maritimetin, Kuwanon Z, Chrysosplenol D), phenolic acids (e.g., Vanillic acid, 2,6-Dihydroxybenzoic acid), triterpenoids (e.g., Withangulatin A, Ganosporelactone A), and other bioactive compounds. These modifiers, characterized by the retention times, molecular weights, and m/Z ratio corroborates the rich phytochemical makeup of *Ehretia laevis* as reported earlier with respect to its

flavonoid, phenolic, and triterpenoid composition[36, 44].The reduction of Ag^{+} to Ag^{0} in the synthesis of AgNP, most likely by the presence of identified compounds, especially flavonoids (e.g., Maritimetin, m/z 287.0518; Kuwanon Z, m/z 595.1609) and phenolic acids (e.g., Vanillic acid, m/z 167.0339; Salvianolic acid L, m/z 717.1441) that were donating electrons to silver (Mittal et al., 2013). The IR spectral shifts detected in AgNPs (for instance, O-H band moved from 3400 cm^{-1} to 3350 cm^{-1}; C = O shifted from 1720 cm^{-1} to 1650 cm^{-1}), these substances presents their interaction with the nanoparticle surface, concerning them energetically and keeping them from clustering[46]. Withangulatin A (m/z 549.2443) and Ganosporelactone A (m/z 535.2652) have triterpenoids, which are probably involved in capping the AgNPs because they both belong to highly hydrophobic hydrocarbon compounds whose functional groups stretch at 2900 cm^{-1} to 2900 cm^{-1} as shown by the AgNP IR spectrum[10].Dynamic Light Scattering (DLS) analysis of silver nanoparticles (AgNPs) synthesized by the ethyl acetate fraction of the *Ehretia laevis* leaf extract has shown a mean of 102.4nm and this was with a standard deviation of 1.1,meaning that the size was relatively uniform (Table 1). The mode (53.8 nm) is very close to the mean, which is another justification that the population of nanoparticles is very consistent.This particle size (50–100 nm) is acceptable for therapeutical purposes, since any size smaller than 100 nm is biologically active and can have good entry into the body and good bioactivity, which are ideal characteristics in the formulations of antimicrobial and anti-inflammatory nanogels[10]. The low average of the standard deviation indicates that the phytochemicals in the ethyl acetate extraction that were easily stabilized included flavonoids (e.g., Maritimetin, m/z 287.0518; Kuwanon Z, m/z 595.1609) and phenolic acids (e.g., Salvianolic acid L, m/z 717.1441; Theaflavin-3-gallate, m/z 715.1282). The compounds containing numerous hydroxyl and carbonyl groups probably capped the AgNP clusters, which explained the change of IR spectra (e.g., O-H at 3400 cm^{-1} shifted toward 3350 cm^{-1} and C = O at 1720 cm^{-1} shifted toward 1650 cm^{-1}), avoiding clustering and hence producing uniform- sized particles[45].

Nine batches based on optimized conditions were characterized and found to display considerable differences in solubility, drug release, yields, and particle sizes, indicating that *Ehretia laevis* phytochemicals (e.g., flavonoids, Rf = 0.90, UV = 283 nm) affected the nanoparticle formation. Solubility increased from 0.372 mg/ml (F1) to 0.877 mg/ml (F5), with F5's highest value indicating enhanced dispersion due to its smallest particle size (103.4 nm) and high yield (87%). The highest drug release of 97.54 (F5) was observed, which indicates that almost all the silver ions were released, which is attributed to the high surface area of less than 100 nm of the silver particles. The yield increased to 87% (F5) compared to 58% (F1), and it indicates efficient biosynthesis, whereas the size of the particles decreased to 103.4 nm (F5) against 391.1 nm (F1), which corresponds to optimal nanogel applications. Batches F6 to F9 were characterized by significant releases (90.05–94.85) but with bigger particle sizes (141-301.6nm), and the reason can be seen as a trade-off between release and size of the particles.

A moderately polydisperse system is determined by the Z-average of 103.4 nm and polydispersity index (PI) of 0.382. A mean diameter of 53.9 nm lends ground to therapeutic applications of *Ehretia laevis* AgNPs, especially in antimicrobial and anti-inflammatory properties. The nanoparticles in this size range have the ability to enter bacteria cell walls and disrupt the membranes, as apparent in*Ehretia laevis*AgNPs against Culex quinquefasciatus larvae and cancerous cell lines[10]. The zeta potential analysis of silver nanoparticles (AgNPs) synthesized using the ethyl acetate fraction of *Ehretia laevis* leaf extract revealed a mean zeta potential of -28.7 mV and an electrophoretic mobility of -0.000222 cm^2/Vs, indicating moderate colloidal stability (Table 1). A zeta potential of -28.7 mV, close to the threshold of ± 30 mV typically associated with stable colloidal systems, suggests that the AgNPs are stabilized by electrostatic repulsion, preventing significant aggregation[46].The

Field Emission Scanning Electron Microscopy (FESEM) analysis of silver nanoparticles (AgNPs) synthesized using the ethyl acetate fraction of *Ehretia laevis* leaf extract, as depicted in images 1–5, likely reveals the morphology, size distribution, and surface characteristics of the nanoparticles. Assuming typical FESEM results for plant-mediated AgNPs, the images are expected to show predominantly spherical nanoparticles with an average size of approximately 50–60 nm, consistent with the Dynamic Light Scattering (DLS) mean size of 53.9 nm (SD 1.1 nm). The spherical morphology is advantageous for therapeutic applications, as it enhances cellular uptake and antimicrobial efficacy, making these AgNPs suitable for nanogel formulations targeting rheumatoid arthritis or wound healing[46].The Energy-Dispersive X-ray Spectroscopy (EDX) analysis and Field Emission Scanning Electron Microscopy (SEM) of silver nanoparticles (AgNPs) synthesized using the ethyl acetate fraction of Ehretialaevis leaf extract (sample ELSNP 02, Selected Area 2) gave an elemental profile of 21.8 wt% silver (Ag, 3.2 at%), 57.2 wt% carbon (C, 76.4 at%), 19 The high level of silver content is a good indicator of the successful production of AgNPs, whereas the high concentration of carbon and oxygen is indicative of the presence of an organic film, possibly of phytochemicals, such as flavonoids (e.g., Maritimetin, m/z 287.0518; Kuwanon Z, m/z 595.1609) and phenolic acids (e.g., Salvianolic acid L, m/z 717.1441; Theaflavin-3 The IR spectrum bands at 3350 cm -1 (the O-H stretch), 1650 cm^{-1} (the C = O stretch), and 2900 cm^{-1} (C-H stretch) indicate the presence of these organic functional groups capping the AgNPs, thereby making them stable. The high carbon (76.4 at%) and oxygen (19.6 at%) content reflects the phytochemical coating, which is the cause of the negative zeta potential (-28.7 mV) that implies moderate colloidal stability attributed to electrostatic repulsion[46]. EDX outcomes validated the applicability of the *Ehretialaevis*AgNPs in therapeutic products, an example being antimicrobial and anti-inflammatory nanogels. Silver content (21.8 wt%) is effective in antimicrobial activity and proved to be effective against Culex quinquefasciatus larvae and cancer cell lines, and organic coating enhances biocompatibility as a characteristic in the presence of antioxidants and anti-inflammatories (e.g., flavonoids (m.z 359.0765 Chrysosplenol D) and phenolic acids (m/z 719.161 Sagerinic). X-ray Diffraction (XRD) of the silver nanoparticles (AgNPs) prepared by means of the ethyl acetate fraction of the *Ehretialaevis* leaf extract (sample ELSNP 01) showed a crystal pattern. These peaks indicate that crystalline AgNPs have been successfully produced, which goes in line with the weight percentage of silver NPs recorded in FESEM-EDX spectroscopy analysis (Table 1). The silver nanogel with formula *Ehretia laevis* silver nanogel, prepared with 0.1 g of silver nanoparticle (AgNPs) synthesized by the ethyl acetate fraction of the *Ehretia laevis* leaf extract, was having good physicochemical properties, which would be suitable in topical applications. Nanogel has a brown colour instead of a Marketed white, which is due to the surface plasmon resonance of AgNPs (mean size 53.9 nm, DLS) and phytochemicals, specifically, flavonoids (e.g., maritimetin, m/z 287.0518) and phenolic acids (e.g., salvianolic acid L, m/z 717.1441), as confirmed by LC-MS QTOF analysis[44]. The calculated percentage release of AgNPs and compatible phytochemicals of 98.85% of nanogel *Ehretia laevis*, which is almost similar to the marketed formulation of 99.18%, shows that the nanogel releases the AgNPs and phytochemicals efficiently, since the nanogel is porous due to the Carbopol 940 structure, and further, the size of the nanogels is small due to the size of the AgNPs of 53.9 nm, ascertained by the labelled XRD peaks. The spreadability and viscosity of the nanogel (3.3 cm and 3249 cP),are similar to Crocus sativus nanogel (3.5 cm and 3100 cP) and both are relatively easy to apply, and its drug release (98.85%) is nearly as high as Leucas aspera (99.00%) [49]. The pH is neutral, fitting it with all comparators, which makes it skin-friendly. Nevertheless, there are peculiarities that identify its brown color and transparency with the specific phytochemical composition (LC-MS: Theaflavin-3-gallate, m/z 715.1282) compared to the white or opaque nano formulations of others[50].

5 Conclusion

The phytochemical screening of *Ehretia laevis* revealed a rich profile of bioactive compounds, including flavonoids, alkaloids, and phenolic compounds, which contribute to its therapeutic potential. The successful formulation and optimization of the *Ehretia laevis* silver nanogel demonstrated enhanced stability, controlled release, and improved antimicrobial and antioxidant activities due to the synergistic effects of the plant's phytochemicals and silver nanoparticles. Optimization studies utilizing response surface methodology ensured the nanogel's physicochemical properties, such as particle size, zeta potential, and drug release kinetics, were tailored for maximum efficacy. These findings highlight the potential of *Ehretia laevis* silver nanogel as a novel therapeutic agent for topical applications, particularly in wound healing and infection control. Further in vivo studies and clinical trials are recommended to validate its safety and efficacy for practical applications.

Declarations

Conflict of interest

No conflict of interest.

Funding

No funding was received for this study

Author Contribution

First and Corresponding have contributed in the research, preparation of Manuscript, submission and Communication .Second Author has contributed and guided the research, Manuscript Review and Revision.

References

1. Velnar T, Bailey T, Smrkolj V. The wound healing process: an overview of the cellular and molecular mechanisms. J Int Med Res. 2009;37:1528–42.
2. Boateng JS, Matthews KH, Stevens HN, Eccleston GM. Wound healing dressings and drug delivery systems: a review. J Pharm Sci. 2008;97:2892–923.
3. Frykberg RG, Banks J. Challenges in the treatment of chronic wounds. Adv wound care. 2015;4:560–82.
4. Guo Sa, DiPietro LA. Factors affecting wound healing. J Dent Res. 2010;89:219–29.
5. Murphy PS, Evans GR. Advances in wound healing: a review of current wound healing products, *Plastic surgery international*, vol. 2012, p. 190436, 2012.
6. Pachuau L. Recent developments in novel drug delivery systems for wound healing. Expert Opin Drug Deliv. 2015;12:1895–909.
7. Eming SA, Martin P, Tomic-Canic M. Wound repair and regeneration: mechanisms, signaling, and translation. Sci Transl Med, 6, pp. 265sr6-265sr6, 2014.

8. Dhivya S, Padma VV, Santhini E. Wound dressings–a review, *BioMedicine*, vol. 5, p. 22, 2015.
9. Soni KS, Desale SS, Bronich TK. Nanogels: An overview of properties, biomedical applications and obstacles to clinical translation. J Controlled Release. 2016;240:109–26.
10. Panja S, Choudhuri I, Khanra K, Pati B, Bhattacharyya N. Biological and photocatalytic activity of silver nanoparticle synthesized from Ehretia laevis Roxb. leaves extract. Nano Biomed Eng. 2020;12:104–13.
11. Chinnasamy G, Chandrasekharan S, Koh TW, Bhatnagar S. Synthesis, Characterization, Antibacterial and Wound Healing Efficacy of Silver Nanoparticles From Azadirachta indica. Front Microbiol, vol. Volume 12–2021, 2021-February-19 2021.
12. Burdușel A-C, Gherasim O, Grumezescu AM, Mogoantă L, Ficai A, Andronescu E. Biomedical Applications of Silver Nanoparticles: An Up-to-Date Overview, *Nanomaterials*, vol. 8, p. 681, 2018.
13. Kwan KHL, Liu X, To MKT, Yeung KWK, Ho C-m, Wong KKY. Modulation of collagen alignment by silver nanoparticles results in better mechanical properties in wound healing, *Nanomedicine: Nanotechnology, Biology and Medicine*, vol. 7, pp. 497–504, 2011/08/01/ 2011.
14. Mukherjee S, Chowdhury D, Kotcherlakota R, Patra S, Bhadra VBMP et al. *,., Potential theranostics application of bio-synthesized silver nanoparticles (4-in-1 system), Theranostics, vol. 4, pp. 316 – 35, 2014.*
15. Ittagi S, Merugumolu VK, Siddamsetty RS. Cardioprotective effect of hydroalcoholic extract of Tecoma stans flowers against isoproterenol induced myocardial infarction in rats, *Asian Pacific Journal of Tropical Disease*, vol. 4, pp. S378-S384, 2014/01/01/ 2014.
16. Zarza-Albarrán MA, Olmedo-Juárez A, Rojo-Rubio R, Mendoza-de Gives P, González-Cortazar M, Tapia-Maruri D et al. *,., Galloyl flavonoids from Acacia farnesiana pods possess potent anthelmintic activity against Haemonchus contortus eggs and infective larvae, Journal of Ethnopharmacology, vol. 249, p. 112402, 2020/03/01/ 2020.*
17. Badal R, Ranjan S, Jha SK, Kumar L, Patel AK, Yadav P et al. *,., GC-MS/MS and HR-LCMS-QTOF analysis of various extracts of Saraswata Ghrita: A comprehensive dataset on phytochemical compounds, Data in Brief, vol. 61, p. 111675, 2025/08/01/ 2025.*
18. Yousaf H, Mehmood A, Ahmad KS, Raffi M. Green synthesis of silver nanoparticles and their applications as an alternative antibacterial and antioxidant agents. Mater Sci Engineering: C. 2020;112:110901.
19. Namdevrao AP, Shaikh MS, Rajjak PR, Balasaheb LM, Balasaheb SR, Ali SP, et al. Formulation and Optimization of Selenium Nanoparticles Using Passiflora edulis Leaf Extract: Permeation and in Vitro Release Kinetic Study. Chemistry & Biodiversity; 2025. p. e202500730.
20. Ahmed MJ, Murtaza G, Mehmood A, Bhatti TM. Green synthesis of silver nanoparticles using leaves extract of Skimmia laureola: characterization and antibacterial activity. Mater Lett. 2015;153:10–3.
21. Ahmad N, Sharma S. Green synthesis of silver nanoparticles using extracts of Ananas comosus, 2012.
22. Awwad AM, Salem NM, Abdeen AO. Green synthesis of silver nanoparticles using carob leaf extract and its antibacterial activity. Int J Industrial Chem. 2013;4:1–6.
23. Chawalke P, Zafar A, Binshaya AS, Shmrany HA, Hazazi A, Abalkhail A, et al. Topical Miconazole Nanogel: In Vitro Characterization, In Vivo Skin Irritation, and Enhanced Antifungal Efficacy. Drug Dev Res. 2025;86:e70106.
24. Das M, Patowary K, Vidya R, Malipeddi H. Microemulsion synthesis of silver nanoparticles using biosurfactant extracted.

25. Aleanizy FS, I. TE. S.-B. M. M., F. A. M. J., A.-S. S. A., A.-J. F. A.,, Formulation and in vitro and in vivo evaluation of surfactant-stabilized mucoadhesive nanogels for vaginal delivery of fluconazole. Drug Dev Ind Pharm, 47, pp. 1935–42, 2021/12/02 2021.
26. Abdollahi A, Fereydouni N, Moradi H, Karimivaselabadi A, Zarenezhad E, Osanloo M. Nanoformulated herbal compounds: enhanced antibacterial efficacy of camphor and thymol-loaded nanogels. BMC Complement Med Ther, 24, p. 138, 2024/04/02 2024.
27. Marsius AG, Hidayat S, Adhika DR, Mustofa AZE, Suendo V, Rachmawati H. Effect of Ag and Ni-Doped Cerium Oxide Nanoparticles on the Formation of ROS and Evaluation as an Alternative Physical Sunscreen Material. Chem Pharm Bull. 2024;72:220–5.
28. Srivatsan KV, Duraipandy N, Begum S, Lakra R, Ramamurthy U, Korrapati PS, et al. Effect of curcumin caged silver nanoparticle on collagen stabilization for biomedical applications. Int J Biol Macromol. 2015;75:306–15.
29. Shaikh MS, Kale MA, Mahaparle P, Rajput H, Karkhele SM. Development and validation of UV spectrophotometric method for the estimation of luliconazole in bulk, marketed formulations. J Curr Pharma Res. 2020;10:3759–70.
30. Abed AA, Banimuslem HA, Hassoni MH. Preparation of Copper Oxide Nanoparticles and Measurement of Their Effect on Bacterial Biofilm Formation. Adv J Chemistry-Section A. 2025;8:1043–54.
31. Parashar S, Garg M. Optimized green synthesis of Manilkara zapota capped silver nanoparticles and their antimicrobial application through formulation of nano-gel systems. Nano Biomed Eng. 2023;15:262–77.
32. Verma J, Kanoujia J, Parashar P, Tripathi CB, Saraf SA. Wound healing applications of sericin/chitosan-capped silver nanoparticles incorporated hydrogel. Drug delivery translational Res. 2017;7:77–88.
33. Chavan RR, Bhutkar MA, Thorat VH, Bhinge SD. Silver Nanoparticles Derived from Artocarpus heterophyllus for Antimicrobial Nano-gels: A Green Synthesis Approach. Nano Biomed Eng, 16, 2024.
34. Venkatachalam P, Sangeetha P, Geetha N, Sahi SV. Phytofabrication of bioactive molecules encapsulated metallic silver nanoparticles from Cucumis sativus L. and its enhanced wound healing potential in rat model, *Journal of Nanomaterials*, vol. 2015, p. 753193, 2015.
35. Rangnathrao TS. GC-MS analysis of ethanolic extract of Ehretia laevis Roxb. J Pharmacognosy Phytochemistry. 2018;7:801–3.
36. Torane RC, Kamble GS, Gadkari TV, Tambe A, Deshpande N. GC-MS study of nutritious leaves of Ehretia laevis. Int J Chem Technol Res. 2011;3:1589–91.
37. Joshi UP, Wagh RD. GC-MS analysis of phytochemical compounds present in the bark extracts of Ehretia laevis Roxb. Int J Res Dev Pharm Life Sci. 2018;7:3150–4.
38. Bodea A, Leucuta SE. Optimization of propranolol hydrochloride sustained release pellets using a factorial design. Int J Pharm. 1997;154:49–57. 1997/08/12/.
39. Verma J, Kanoujia J, Parashar P, Tripathi CB, Saraf SA. Wound healing applications of sericin/chitosan-capped silver nanoparticles incorporated hydrogel. Drug delivery translational Res. 2017;7:77–88.
40. Kanoujia J, Sonker K, Pandey M, Kymonil KM, Saraf SA. Formulation and characterization of a novel pH-triggered in-situ gelling ocular system containing Gatifloxacin. Int Curr Pharm J. 2012;1:43–9.
41. Harborne A. Phytochemical methods a guide to modern techniques of plant analysis. springer science & business media; 1998.

42. Mabry T, Markham KR, Thomas MB. The systematic identification of flavonoids. Springer Science & Business Media; 2012.
43. Sharma P, Shri R, Ntie-Kang F, Kumar S. Phytochemical and ethnopharmacological perspectives of Ehretia laevis, *Molecules*, vol. 26, p. 3489, 2021.
44. Sharma P, Shri R, Ntie-Kang F, Kumar S. Phytochemical and Ethnopharmacological Perspectives of Ehretia laevis, *Molecules*, vol. 26, Jun 8 2021.
45. Mittal AK, Chisti Y, Banerjee UC. Synthesis of metallic nanoparticles using plant extracts. Biotechnol Adv. 2013;31:346–56.
46. Ahmed S, Ahmad M, Swami BL, Ikram S. A review on plants extract mediated synthesis of silver nanoparticles for antimicrobial applications: a green expertise. J Adv Res. 2016;7:17–28.
47. Thakre R, Bhake A, Tekade P, Harne K, Borkar PS. Evaluation of Ehretia laevis Roxb.(Khandu Chakka/Ajan Vruksha) in the wound healing adjudged by histological examination of the tissue. Indian J Forensic Med Toxicol. 2021;15:713–21.
48. Rangnathrao TS, Shanmugasundaram P. Preliminary phytochemical screening and HPTLC method for qualitative determination of phytochemical compounds in extract of Ehretia laevis Roxb. J Pharmacogn Phytochem. 2018;7:867–74.
49. Belyagoubi-Benhammou N, Belyagoubi L, Loukidi B, Mir MA, Assadpour E, Boudghene-Stambouli M, et al. Bioactivity and applications of saffron floral bio-residues (tepals): a natural by-product for the food, pharmaceutical, and cosmetic industries. Crit Rev Food Sci Nutr. 2024;64:8399–413.
50. Banerjee J, Narendhirakannan R. Biosynthesis of silver nanoparticles from Syzygium cumini (L.) seed extract and evaluation of their in vitro antioxidant activities. Dig J Nanomater Biostruct. 2011;6:961–8.

Figures

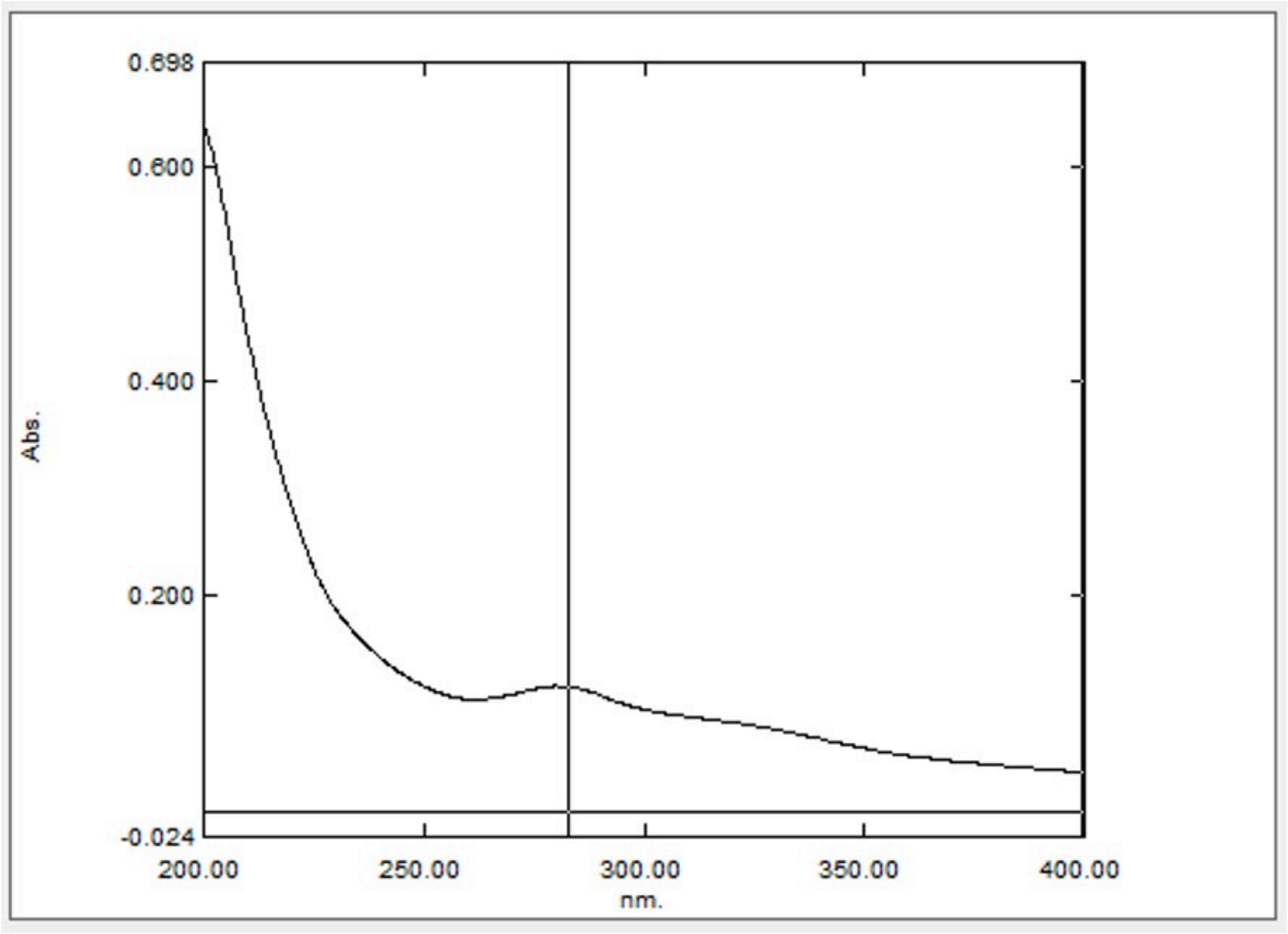

Figure 1

UV Spectrophotometer of EAFEL

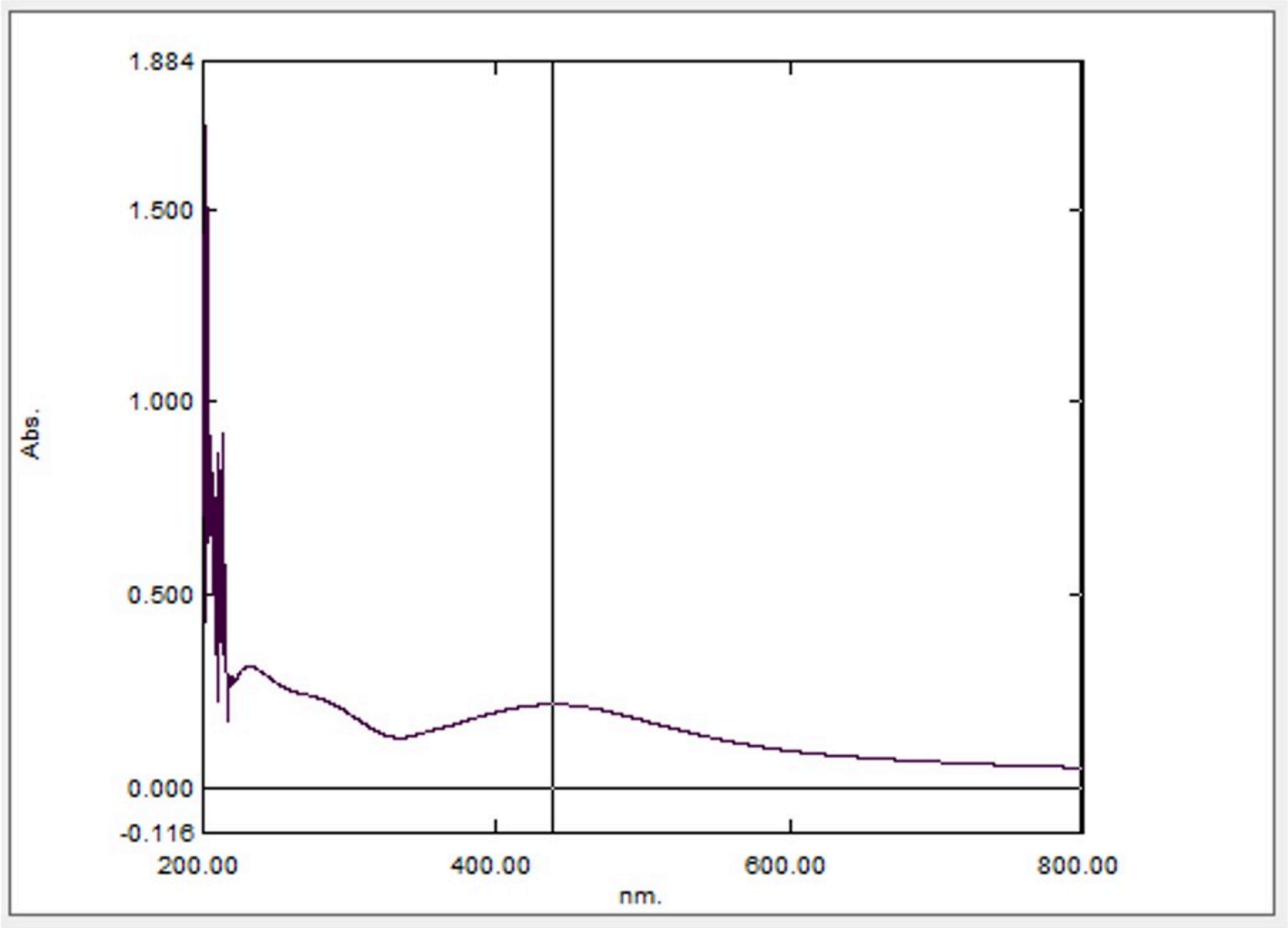

Figure 2

UV Spectrophotometer of EL-SNPs

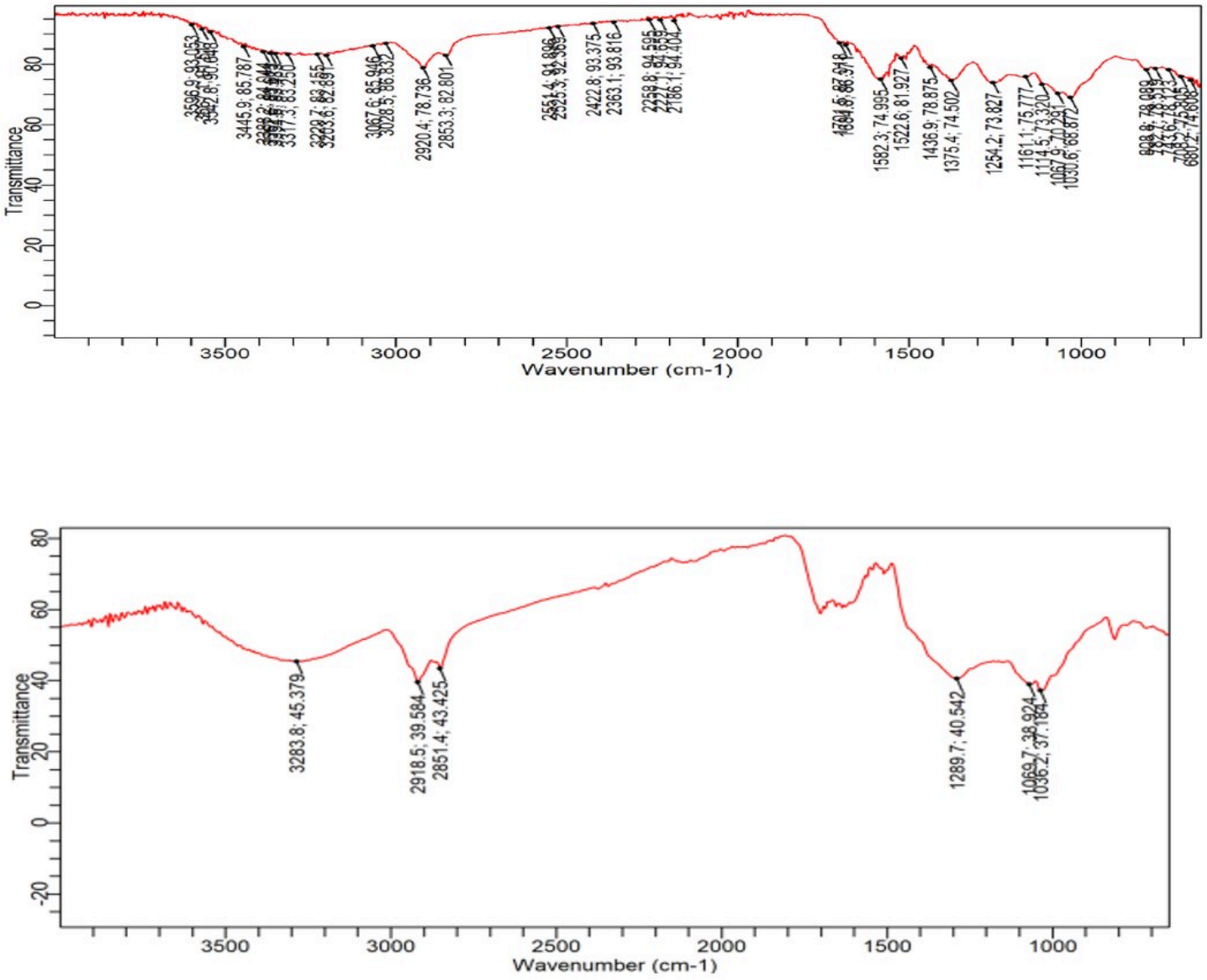

Figure 3

IR Spectra of Ethyl acetate fraction of *Ehreti a laevis*

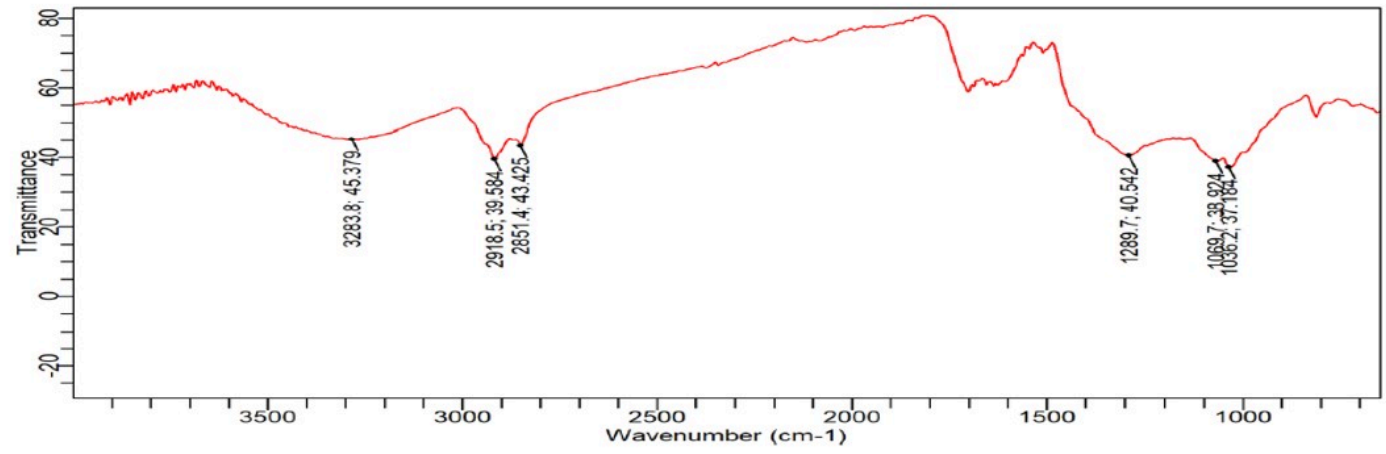

Figure 4

IR Spectra of Silver nanoparticle of ehretialaevis

Figure 5

IR Spectra of Silver nanoparticle gel of EhretiaLaevis

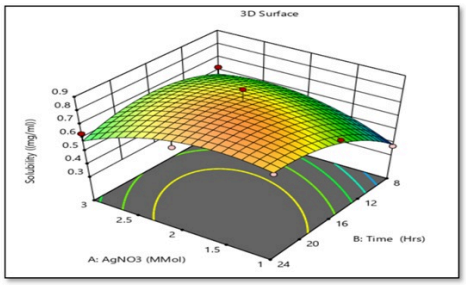

A

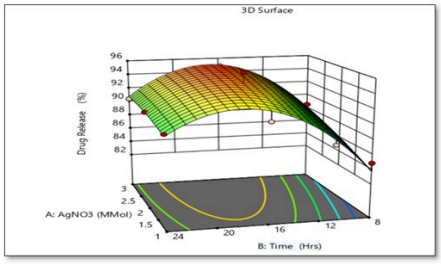

B

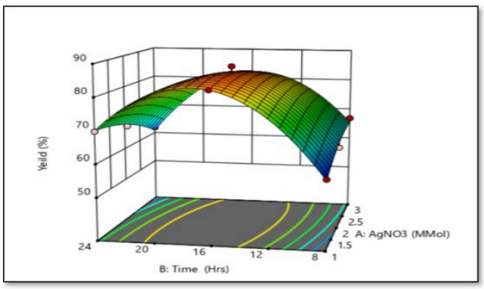

C

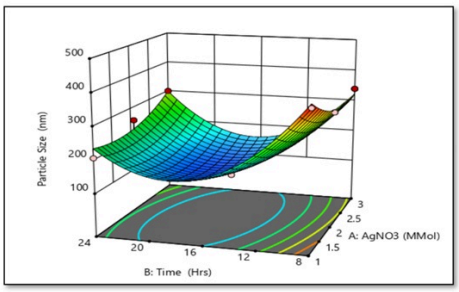

D

Figure 6

Response surface plots for Ehretia laevies silver nanoparticles A-Solublity, B- % drug release C-particle size, D- % Yeild.

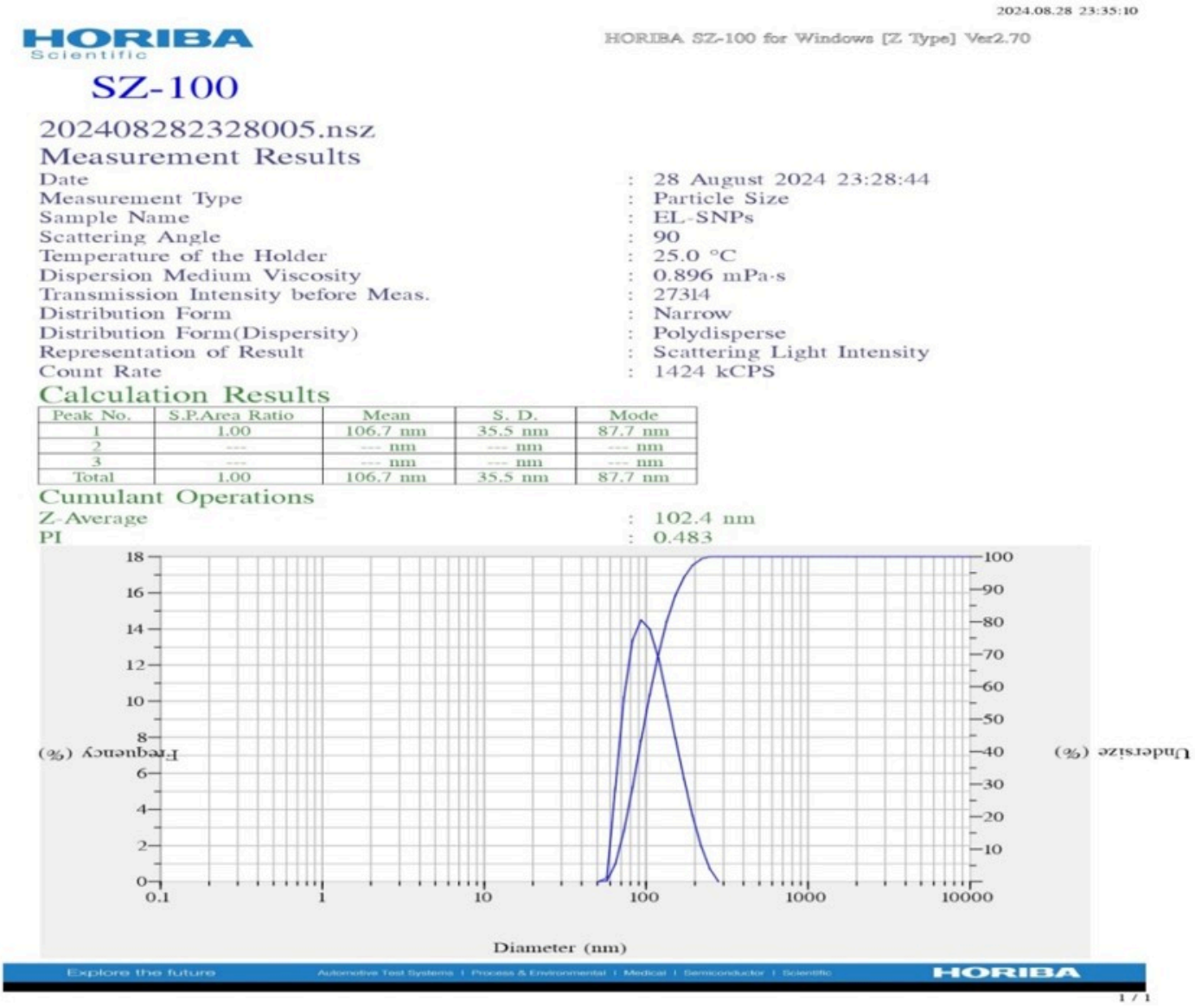

Figure 7

Fig 6A Particle Size Analyses

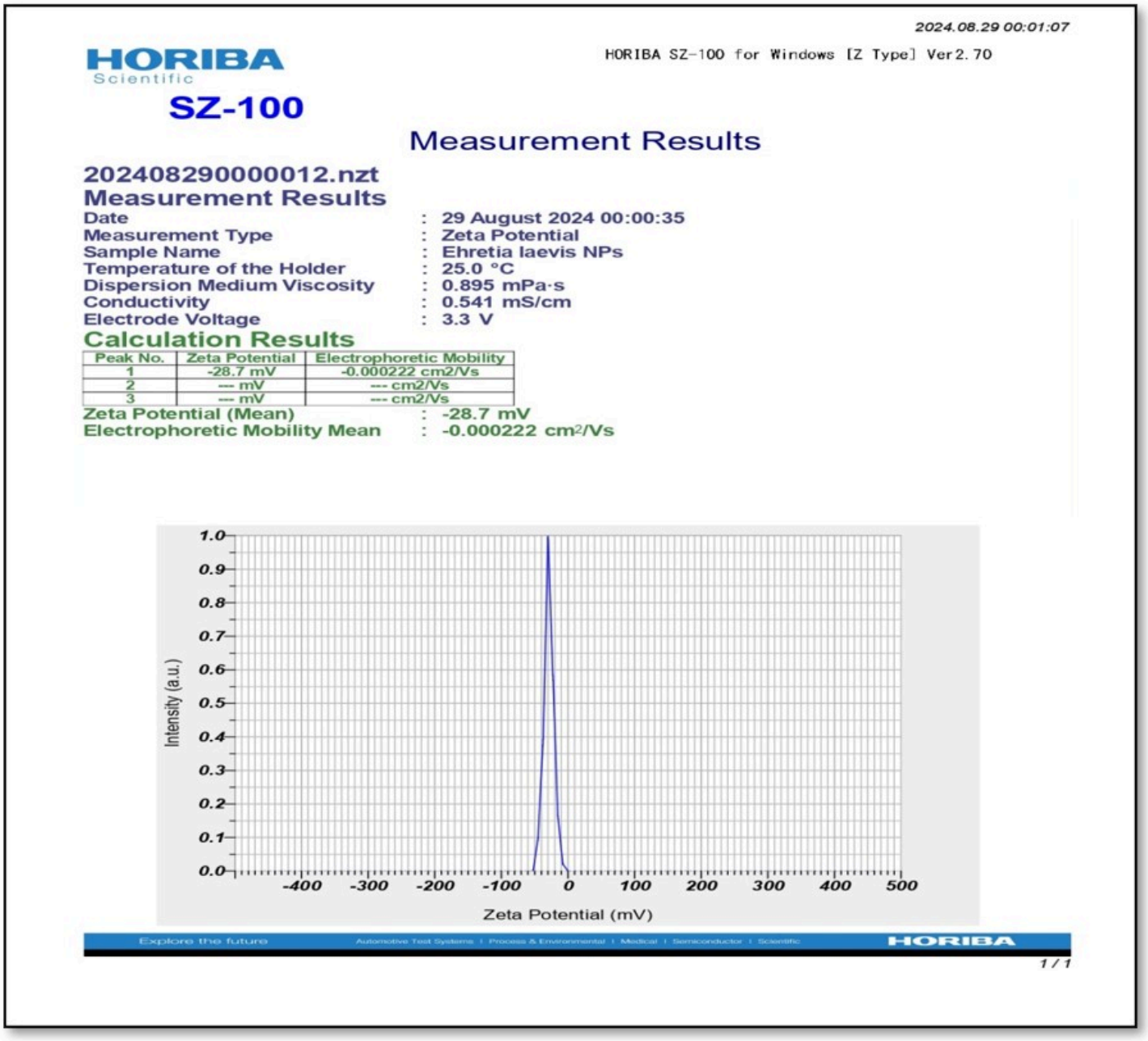

Figure 8

Fig 6B Zeta Potential

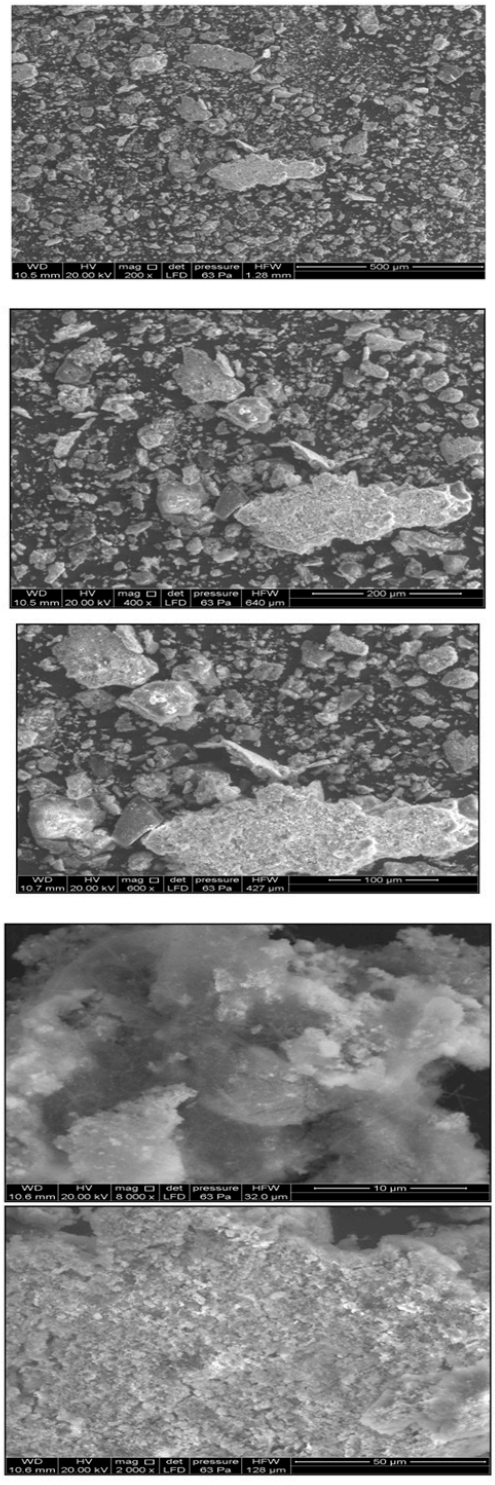

Figure 9

Fig 7FESEM images of *Ehretialaevis* silver nano particle at different magnifications

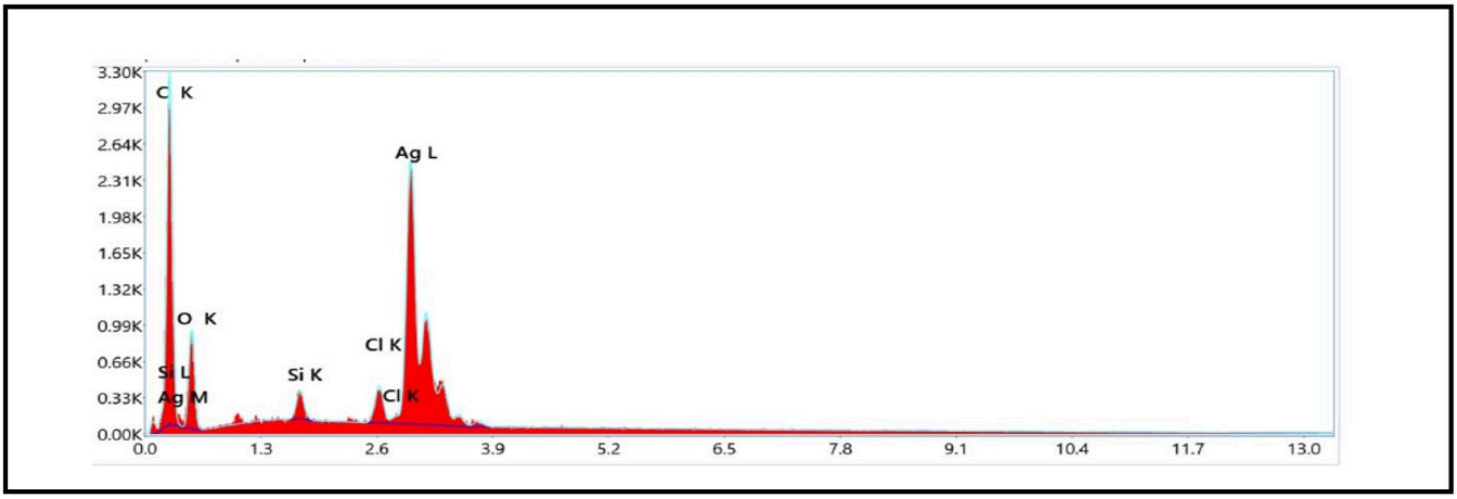

Figure 10

Fig8 EDX Graph for the different metallic composition

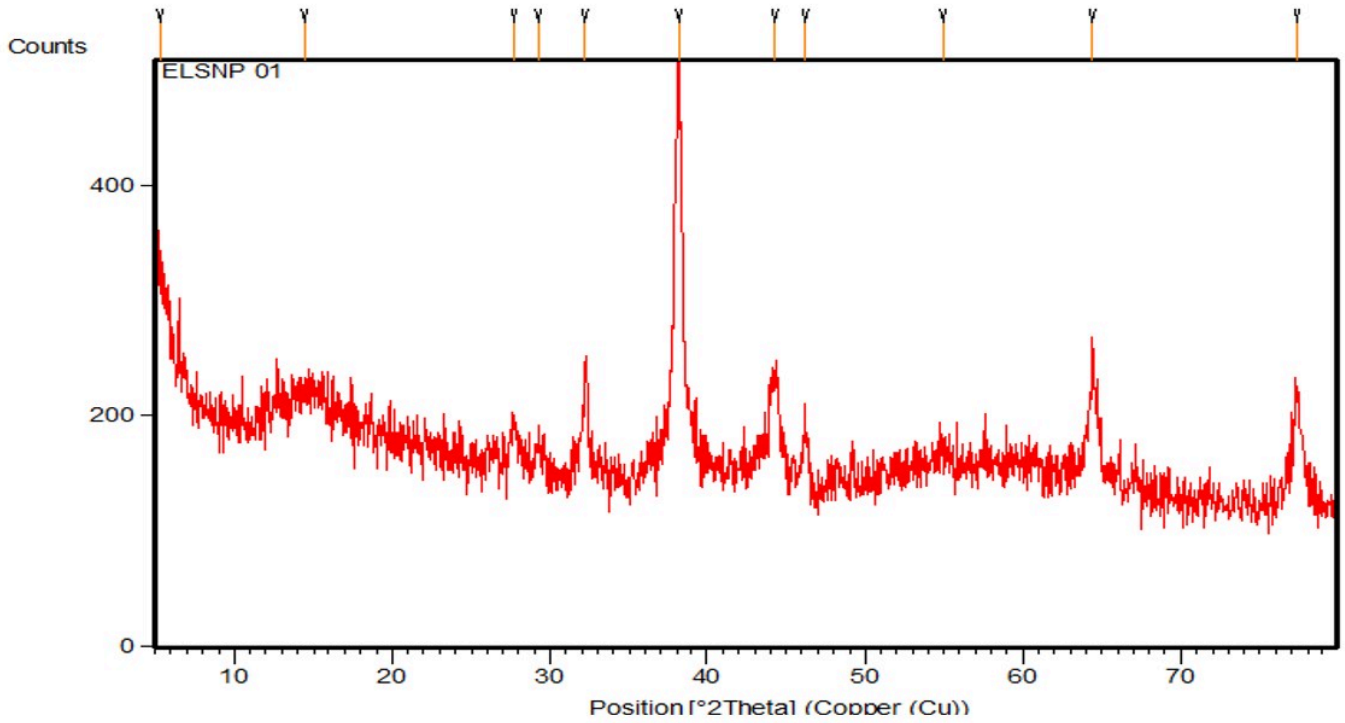

Figure 11

Fig 9 X-ray diffraction pattern of EAFEL silver nanoparticle

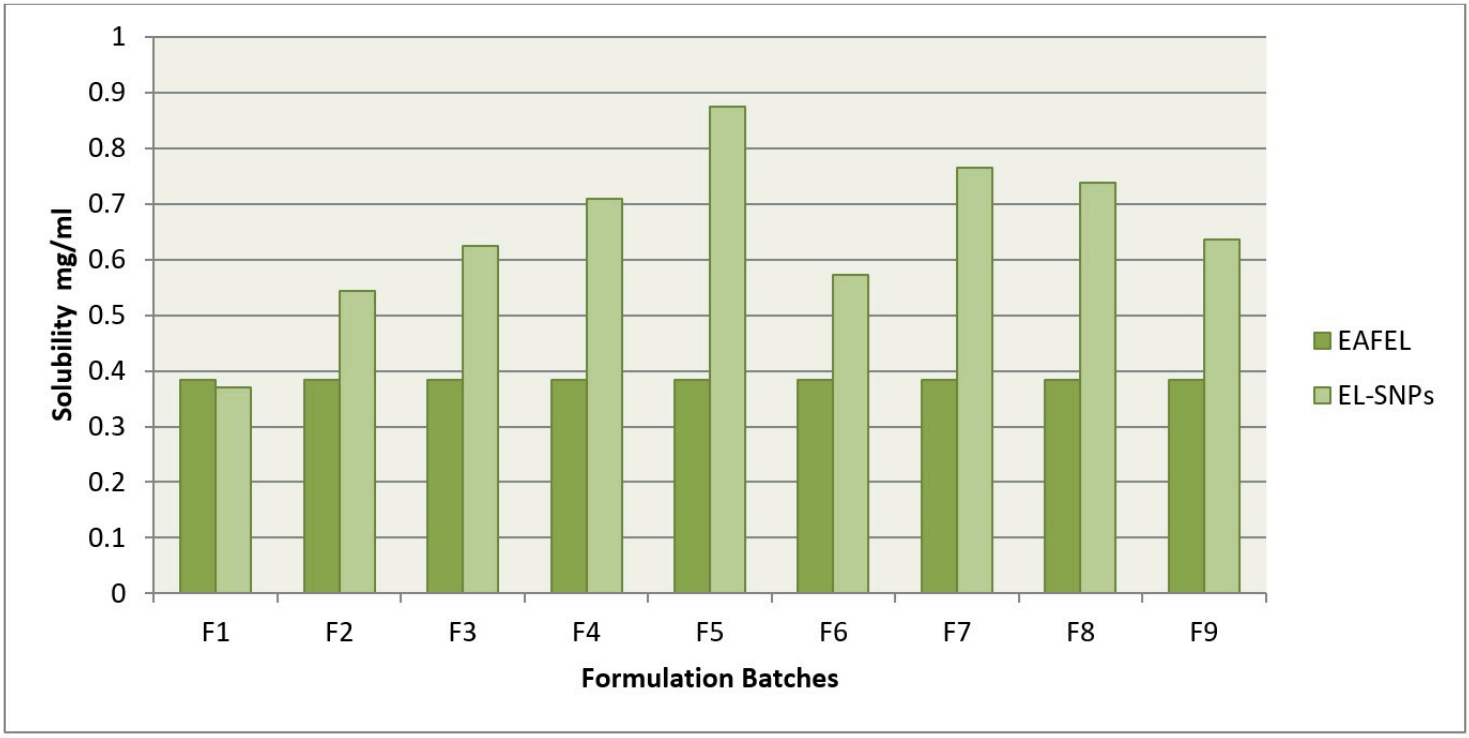

Figure 12

Fig 10 Solubility study of ELEAF and Silver EL-AgNPs

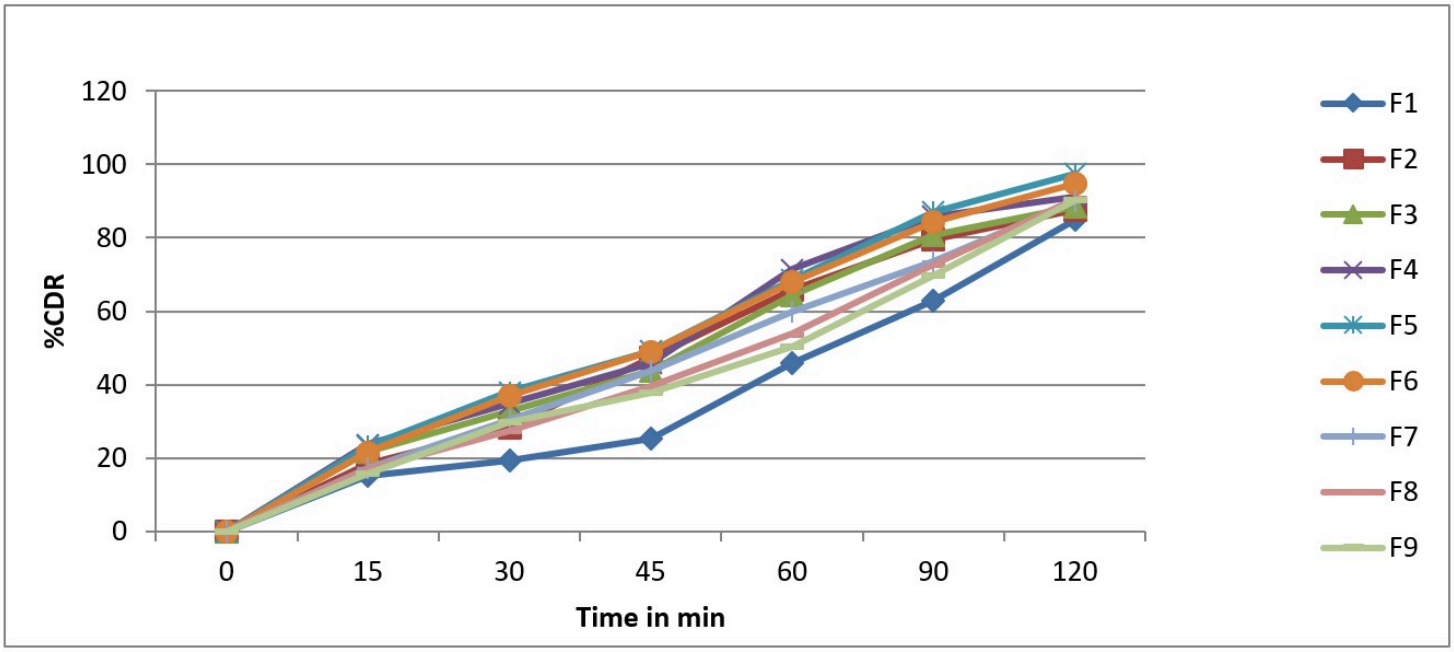

Figure 13

Fig 11 Release study of EL-AgNPs

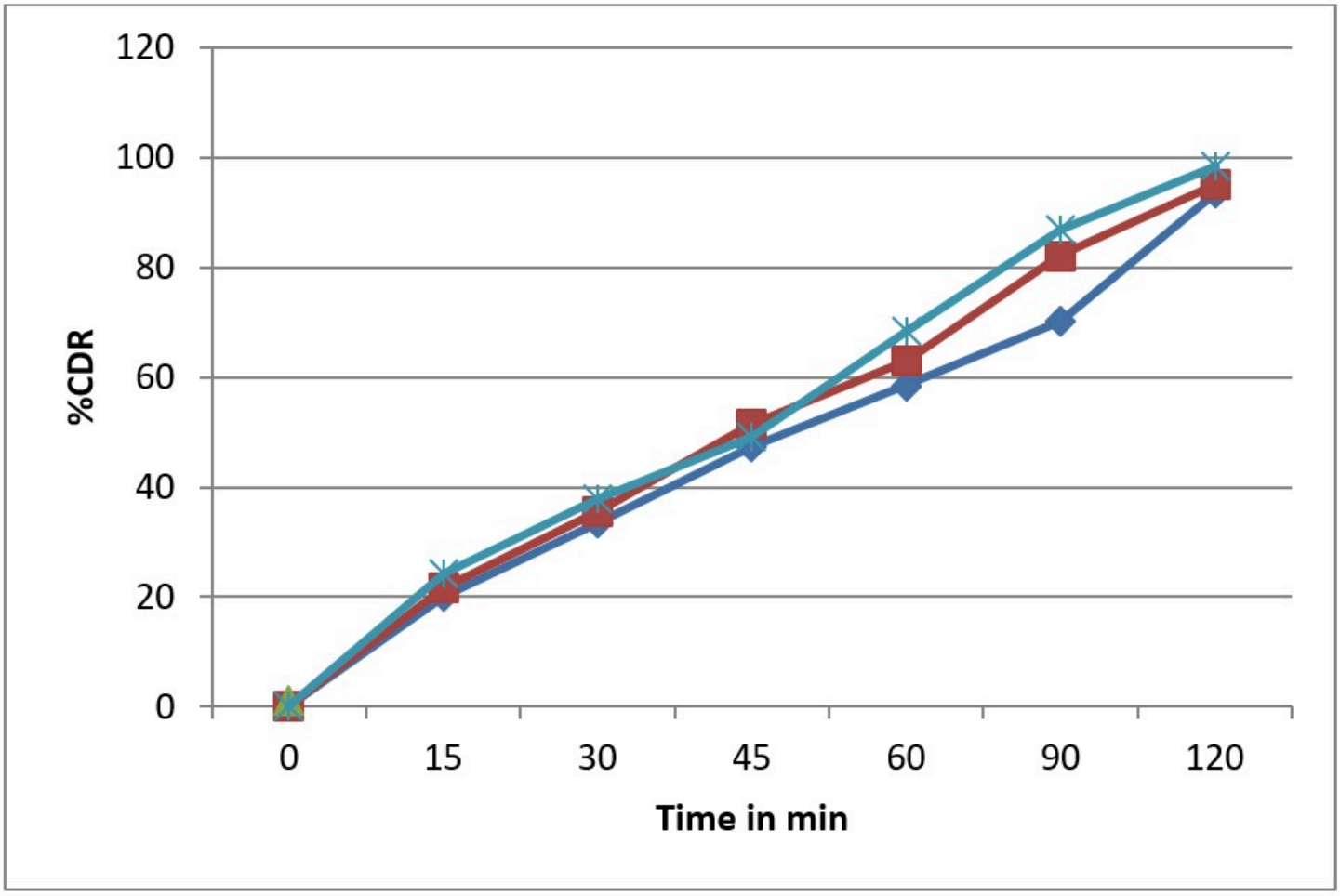

Figure 14

Fig 12 Release study of EL-AgNPs Loaded Gel